

CAPITAL UNIVERSITY OF SCIENCE AND  
TECHNOLOGY, ISLAMABAD



**A Deep Learning Framework for  
Classification of Intracranial  
Hemorrhage Subtypes with  
Attention-Based Approaches**

by

**Memoona Zulfiqar**

A thesis submitted in partial fulfillment for the  
degree of Master of Science

in the

**Faculty of Computing**

**Department of Computer Science**

2023

Copyright © 2023 by Memoona Zulfiqar

All rights reserved. No part of this thesis may be reproduced, distributed, or transmitted in any form or by any means, including photocopying, recording, or other electronic or mechanical methods, by any information storage and retrieval system without the prior written permission of the author.

*My dissertation work is devoted to My Family, My Teachers, and My Friends. I have a special feeling of gratitude for My beloved parents and brothers. Special thanks to my supervisor whose uncountable confidence enabled me to reach this milestone.*




## CERTIFICATE OF APPROVAL

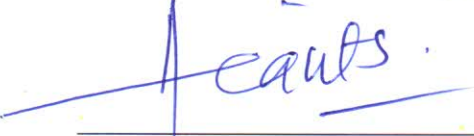
### A Deep Learning Framework for Classification of Intracranial Hemorrhage Subtypes with Attention-Based Approaches

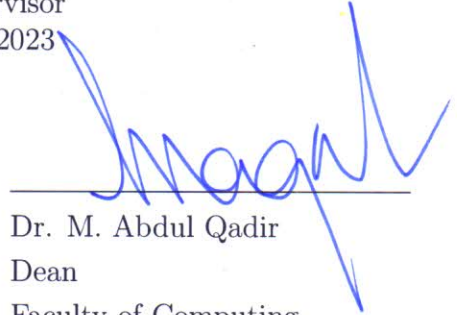
by  
Memoona Zulfiqar  
(MCS213004)

### THESIS EXAMINING COMMITTEE

S. No.	Examiner	Name	Organization
(a)	External Examiner	Dr. Ayyaz Hussain	QAU, Islamabad
(b)	Internal Examiner	Dr. Nadeem Anjum	CUST, Islamabad
(c)	Supervisor	Dr. Abdul Basit Siddiqui	CUST, Islamabad

  
\_\_\_\_\_  
Dr. Abdul Basit Siddiqui  
Thesis Supervisor  
November, 2023

  
\_\_\_\_\_  
Dr. Abdul Basit Siddiqui  
Head  
Dept. of Computer Science  
November , 2023

  
\_\_\_\_\_  
Dr. M. Abdul Qadir  
Dean  
Faculty of Computing  
November, 2023

## *Author's Declaration*

I, **Memoona Zulfiqar** hereby state that my MS thesis titled “**A Deep Learning Framework for Classification of Intracranial Hemorrhage Subtypes with Attention-Based Approaches**” is my own work and has not been submitted previously by me for taking any degree from Capital University of Science and Technology, Islamabad or anywhere else in the country/abroad.

At any time if my statement is found to be incorrect even after my graduation, the University has the right to withdraw my MS Degree.



(Memoona Zulfiqar)

Registration No: MCS213004

---

## *Plagiarism Undertaking*

I solemnly declare that research work presented in this thesis titled “**A Deep Learning Framework for Classification of Intracranial Hemorrhage Subtypes with Attention-Based Approaches**” is solely my research work with no significant contribution from any other person. Small contribution/help wherever taken has been duly acknowledged and that complete thesis has been written by me.

I understand the zero tolerance policy of the HEC and Capital University of Science and Technology towards plagiarism. Therefore, I as an author of the above titled thesis declare that no portion of my thesis has been plagiarized and any material used as reference is properly referred/cited.

I undertake that if I am found guilty of any formal plagiarism in the above titled thesis even after award of MS Degree, the University reserves the right to withdraw/revoke my MS degree and that HEC and the University have the right to publish my name on the HEC/University website on which names of students are placed who submitted plagiarized work.



(Memoona Zulfiqar)

Registration No: MCS213004

## *Acknowledgement*

I am deeply grateful to Almighty Allah for blessing me with knowledge, strength, courage, and patience throughout my studies. I am also very grateful to my supervisor, **Dr. Abdul Basit Siddiqui**, for his close monitoring of the progress of this thesis, providing insights at every stage and correcting the direction whenever necessary.

I would like to express my deepest gratitude to my dearest family members: my father, my mother, and my siblings, for their unconditional support during good times and bad. They have always encouraged me to stay motivated and reach my goals.

I would also like to thank everyone who has helped me along the way. Special thanks to **Mr. Hashim Ayub** for increasing my knowledge and helping me with technical aspects & giving motivational support throughout my research journey.

**(Memoona Zulfiqar)**

# *Abstract*

Intracranial hemorrhages pose a critical threat to patient health, demanding swift and accurate diagnosis. Computed Tomography (CT) scans serve as vital tools for medical professionals to detect and classify hemorrhage subtypes, aiding in timely treatment decisions. However, manual interpretation of CT images is challenging, and existing automated methods have their limitations.

This study presents an innovative approach based on the Attention U-Net model to address the classification of intracranial hemorrhage subtypes. The Attention U-Net combines the strengths of Convolutional Neural Networks (CNNs) and attention mechanisms to efficiently identify and classify brain hemorrhages. The model encompasses an encoder-decoder architecture, with attention mechanisms guiding the decoder to focus on the most pertinent regions of the image.

The methodology involves data preprocessing, augmentation, feature extraction with attention gates, image segmentation, and ultimately, classification of intracranial hemorrhage subtypes on CT scans. Two datasets were employed, each with its unique characteristics, posing significant challenges related to class imbalance and label mutual exclusivity.

Results showcase the model's effectiveness, with improvements in the average F1-score and accuracy, outperforming benchmark techniques. The proposed Attention U-Net model exhibits promise as a valuable tool for medical professionals in the diagnosis and classification of intracranial hemorrhages, paving the way for enhanced patient care and outcomes. Future work may involve further refinement, real-time application, and integration into healthcare systems to augment medical decision-making.



# Contents

<b>Author’s Declaration</b>	<b>iv</b>
<b>Plagiarism Undertaking</b>	<b>v</b>
<b>Acknowledgement</b>	<b>vi</b>
<b>Abstract</b>	<b>vii</b>
<b>List of Figures</b>	<b>x</b>
<b>List of Tables</b>	<b>xi</b>
<b>Abbreviations</b>	<b>xii</b>
<b>1 Introduction</b>	<b>1</b>
1.1 Hemorrhage Background . . . . .	1
1.1.1 Brain Hemorrhage . . . . .	4
1.1.1.1 Subarachnoid Hemorrhage . . . . .	6
1.1.1.2 Subdural Hemorrhage . . . . .	7
1.1.1.3 Epidural Hemorrhage . . . . .	7
1.1.1.4 Intraparenchymal Hemorrhage . . . . .	7
1.1.1.5 Intraventricular Hemorrhage . . . . .	8
1.2 Computer-Aided Diagnosis(CAD) System for Intracranial Hemorrhage Classification . . . . .	8
1.3 Methods Used for Intracranial Hemorrhage Classification. . . . .	11
1.4 Motivation . . . . .	15
1.5 Problem Statement . . . . .	16
1.6 Significant of the Solution . . . . .	17
1.7 Research Questions . . . . .	17
1.8 Thesis Organization . . . . .	18
<b>2 Literature Review</b>	<b>19</b>
2.1 Survey of Existing Techniques . . . . .	19
2.2 Research Gap . . . . .	28
<b>3 Methodology</b>	<b>29</b>

---

3.1	Dateset	33
3.1.1	Challenges	36
3.2	Data Pre-Processing	38
3.3	Proposed Model	42
3.3.1	Model Component	43
3.4	Classification	49
3.5	Benchmark Techniques	51
3.5.1	Mobile-Net	51
3.5.2	Dense-Net 121	53
3.5.3	Dense-Net 169	54
3.5.4	ResNet 101	55
3.5.5	ResNet 152	57
3.6	Evaluation	58
<b>4</b>	<b>Implementation and Experiments of the Proposed Methodology</b>	<b>61</b>
4.1	Tools and Technology	61
4.2	Dataset	63
4.3	Implementation of Model	67
4.4	Classification	69
4.5	Analysis of Result	70
4.6	Model Performance Analysis	74
4.7	Comparative Analysis	76
<b>5</b>	<b>Conclusion and Future Work</b>	<b>78</b>
5.1	Conclusion	78
	<b>Bibliography</b>	<b>80</b>

# List of Figures

1.1	Stroke Types . . . . .	2
1.2	Hemorrhage Types . . . . .	4
1.3	Subtypes of Intracranial Hemorrhage . . . . .	6
1.4	Brain Hemorrhage Classification using Computer-Aided Diagnosis System . . . . .	10
1.5	Schema of Feature Learning-Based Method for Intracranial Hemorrhage (ICH). . . . .	13
1.6	A Deep Learning Model Structure for Intracranial Hemorrhage Classification . . . . .	15
3.1	Proposed Methodology . . . . .	31
3.2	Flowchart of Proposed Methodology . . . . .	32
3.3	Epidural Hemorrhage(EDH) . . . . .	33
3.4	Intraparenchymal Hemorrhage (IPH) . . . . .	34
3.5	Subdural Hemorrhage (SDH) . . . . .	34
3.6	Subarachnoid Hemorrhage (SAH) . . . . .	35
3.7	Intraventricular Hemorrhage (IVH) . . . . .	35
3.8	Attention U-NET for Classification . . . . .	45
3.9	MobileNet Model Diagram . . . . .	52
3.10	DenseNet121 Model Diagram . . . . .	54
3.11	DenseNet-169 Model Diagram . . . . .	55
3.12	ResNet-101 Model Diagram . . . . .	56
3.13	ResNet-152 Model Diagram . . . . .	58
4.1	Class-wise Distribution . . . . .	64
4.2	of the data frame where hemorrhage in the image . . . . .	65
4.3	Balance Dataset1 . . . . .	66
4.4	Balance Dataset2 . . . . .	67
4.5	Train and Validation Learning Curves . . . . .	69
4.6	dataset 1 F-Score of different Techniques . . . . .	71
4.7	dataset 2 F-Score of different Techniques . . . . .	71
4.8	dataset 1 Accuracy of different Techniques . . . . .	72
4.9	dataset 2 Accuracy of different Techniques . . . . .	72
4.10	Dataset 1 Model Performance with different Techniques . . . . .	75
4.11	Dataset 2 Model Performance with different Techniques . . . . .	76

# List of Tables

2.1	Analysis of Existing Techniques . . . . .	26
3.1	Intracranial Hemorrhage Dataset 1 . . . . .	37
3.2	Intracranial Hemorrhage Dataset 2 . . . . .	37
3.3	Intracranial Hemorrhage Balance Dataset 1 . . . . .	38
3.4	Intracranial Hemorrhage Balance Dataset 2 . . . . .	38
4.1	Model Parameter . . . . .	68
4.2	Class Wise Result of Dataset 1 . . . . .	70
4.3	Class Wise Result of Dataset 2 . . . . .	70
4.4	Comparison of Attention UNet Model using Dataset 1 . . . . .	74
4.5	Comparison of Attention UNet Model using Dataset 2 . . . . .	74
4.6	Comparative Analysis with Current Approaches . . . . .	77

# Abbreviations

<b>ACC</b>	Accuracy
<b>AG</b>	Attention Gate
<b>Avg</b>	Average
<b>BSB</b>	Brain-Subdural-Soft Tissues
<b>CAD</b>	Computer-Aided Diagnosis
<b>CNN</b>	Convolutional Neural Network
<b>CPU</b>	Central Processing Unit
<b>CSV</b>	Comma-Separated Values
<b>CT Scan</b>	Computed Tomography Scan
<b>DICOM</b>	Digital Imaging and Communications in Medicine
<b>EDH</b>	Epidural Hemorrhage
<b>F1</b>	F1-Score
<b>GPU</b>	Graphics Processing Unit
<b>GRU</b>	Gated Recurrent Unit
<b>HU</b>	Hounsfield Units
<b>ICH</b>	Intracranial Hemorrhage
<b>IoU</b>	Intersection over Union
<b>IVH</b>	Intraventricular Hemorrhage
<b>JSON</b>	JavaScript Object Notation
<b>LSTM</b>	Long Short-Term Memory
<b>MRI</b>	Magnetic Resonance Imaging
<b>ReLU</b>	Rectified Linear Unit
<b>RNN</b>	Recurrent Neural Network
<b>ROI</b>	Region of Interest

<b>RSNA</b>	Radiological Society of North America
<b>SAH</b>	Subarachnoid Hemorrhage
<b>SDH</b>	Subdural Hemorrhage
<b>SVM</b>	Support Vector Machine
<b>TPR</b>	True Positive Rate
<b>TNR</b>	True Negative Rate

# Chapter 1

## Introduction

### 1.1 Hemorrhage Background

A stroke occurs when there is a disruption in the normal blood flow to the brain, which can be caused by either a burst blood vessel leading to bleeding within the brain or a blockage that impedes the blood supply to the brain. This disruption in blood flow prevents the brain's tissues from receiving the necessary oxygen and nutrients. The prevailing cause often involves a clot forming within an artery that provides blood to the brain[1]. Alternatively, it can stem from a hemorrhage, arising when a ruptured vessel results in the seepage of blood into the brain. Stroke has the potential to inflict enduring harm, leading to lasting consequences such as partial paralysis and difficulties in speech, understanding, and memory[1, 2]. A stroke is a serious medical condition that can cause sudden and lasting brain damage. Stroke symptoms can vary, encompassing signs such as weakness or paralysis affecting one side of the face or body, a sudden and intense headache, difficulties in speech or comprehension, and visual impairments. According to data from the World Health Organization, On a global scale, it is estimated that 25% of adults aged 25 and above will encounter a stroke during their lifetime. The current year is projected to witness 12.2 million individuals worldwide facing their initial stroke, leading to a tragic outcome for 6.5 million of them. Impressively, the number of individuals who have been impacted by stroke across the globe

surpasses 110 million. According to data from the World Health Organization, the age-standardized death rate attributed to stroke in Pakistan stands at 108.8 per 100,000 individuals. Stroke holds a significant position among the leading causes of mortality in Pakistan[2].

There are two main types of stroke are shown in Figure 1.1:

1. **Ischemic:**In the context of an ischemic stroke, the impediment of blood flow to the brain, often caused by a clot or other barriers, results in a critical interruption of oxygen and nutrient supply to brain cells and tissues. This urgent and time-sensitive situation underscores the importance of prompt medical intervention to restore blood flow and mitigate the severe consequences associated with ischemic strokes.[1–3].
2. **Hemorrhage:** Hemorrhagic strokes transpire when a blood vessel in the brain ruptures, releasing blood into the brain tissue. Consequently, brain cells and tissues may experience oxygen and nutrient deprivation, resulting in harm or demise. Moreover, the hemorrhage can induce an increase in pressure within the brain, exacerbating damage to brain tissue [1–3].

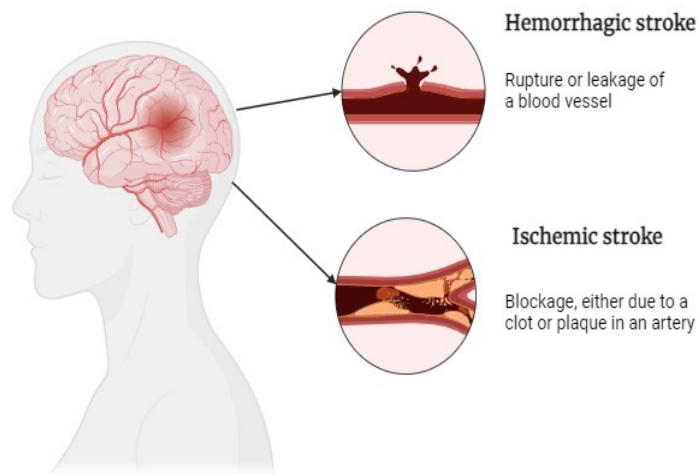


FIGURE 1.1: Stroke Types



Hemorrhage is the medical term for bleeding. It can occur inside or outside the body, and the amount of blood loss can vary from minor to major. Hemorrhage is divided into two types internal and external hemorrhage. When blood spills inside the body, internal bleeding happens. Numerous things, including accidents, surgeries, and illnesses like high blood pressure or blood clotting problems, can contribute to its occurrence. Internal hemorrhage poses a serious risk of death since it can cause a quick loss of blood and a drop in blood pressure. When blood flows outside the body, it causes an external hemorrhage. It frequently results from wounds including cuts, scratches, and puncture wounds. External bleeding can be dangerous, but it usually poses no danger to life[3, 4].

Several other types of hemorrhage can be classified based on their location or cause. These are Brain, Eyes, Nose, Mouth, Lungs, Gastrointestinal tract, Urinary tract, Gynecologic tract, Anus, and Vascula. Different types of hemorrhage are shown in Figure 1.2.

Brain hemorrhage refers to internal bleeding within the brain, categorized into three distinct types: Intracranial hemorrhage, involving bleeding inside the skull; Cerebral hemorrhage, characterized by bleeding within the brain tissue; and Intracerebral hemorrhage, resulting from the rupture of blood vessels within the brain. Eyes can experience Subconjunctival hemorrhage, characterized by bleeding in the white part of the eye. The nose has an Epistaxis hemorrhage(Nosebleed). The mouth has three types of hemorrhage. Tooth eruption(Bleeding when a tooth is lost), Hematemesis(Vomiting blood), and Hemoptysis(Coughing up blood). Bleeding in the lungs is known as Pulmonary hemorrhage. The gastrointestinal tract has three types of hemorrhage Upper gastrointestinal Hemorrhage (Bleeding in the upper part of the gastrointestinal tract, such as the stomach or the esophagus), Lower gastrointestinal hemorrhage( Bleeding in the lower part of the gastrointestinal tract, such as the intestines or the rectum), and Occult gastrointestinal hemorrhage( Bleeding in the gastrointestinal tract that is not visible to the naked eye). Hematuria hemorrhage is caused by Blood in the urine. Gynecologic tract has Vaginal hemorrhage( Bleeding from the vagina.), Postpartum hemorrhage( Bleeding after childbirth), Breakthrough hemorrhage( Bleeding between menstrual

periods), and Ovarian bleeding( Bleeding from the ovaries). In the anus, hemorrhages manifest as Melena, which leads to black, tarry stools due to bleeding in the upper gastrointestinal tract, and Hematochezia, characterized by bright red blood in stool resulting from lower gastrointestinal tract bleeding. Vascular hemorrhages comprise Ruptured aneurysm, where a blood vessel bulge bursts; Aortic transection, marked by a tear in the aorta, the body's primary artery; and Iatrogenic injury, which results from medical treatment[4–6].

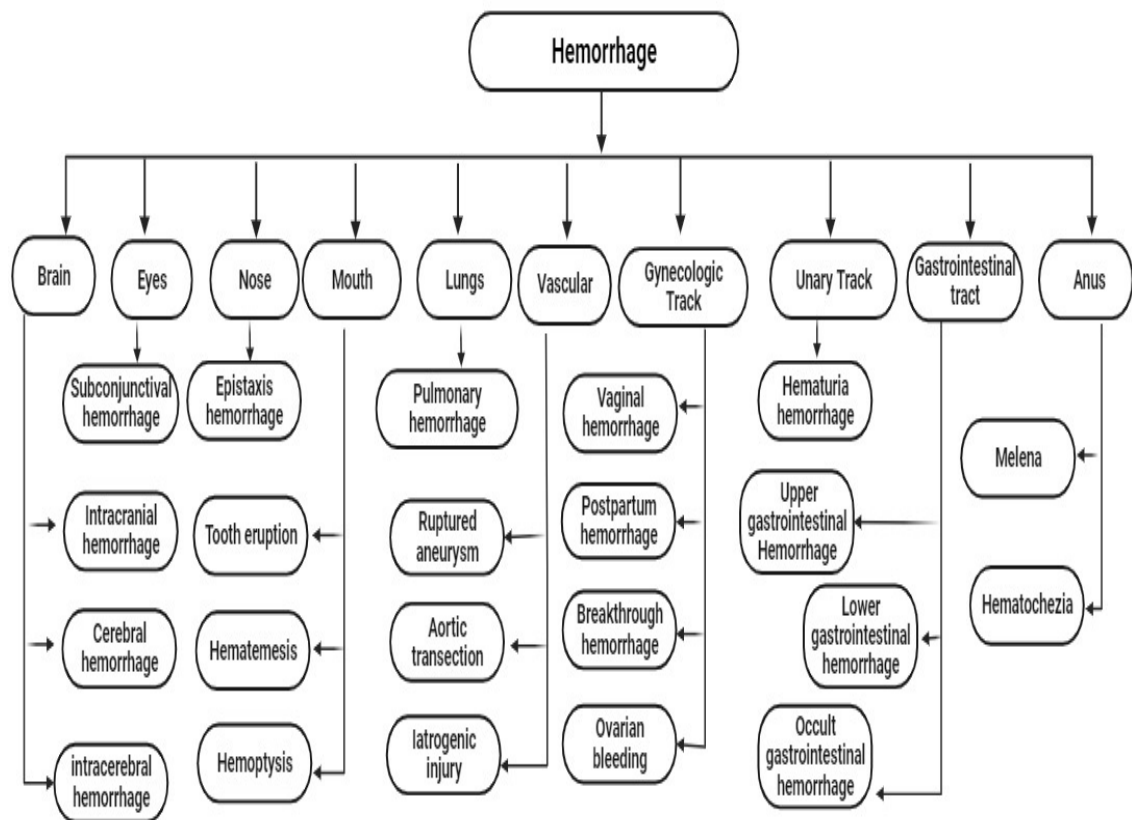


FIGURE 1.2: Hemorrhage Types

### 1.1.1 Brain Hemorrhage

Internal bleeding of the brain is known as Brain Hemorrhage. Brain hemorrhage, also known as intracranial hemorrhage (ICH) refers to a condition where a blood vessel within the brain ruptures, leading to the release of blood into the brain

tissue. These blood vessels can rupture due to high blood pressure, abnormal development, or trauma. When a blood vessel ruptures, blood can leak into the brain tissue, damaging it. Additionally, the presence of excess blood within the brain can elevate the pressure inside the skull, known as intracranial pressure, which can further damage the brain tissue. Intracranial hemorrhage can be a serious medical issue with potentially life-threatening consequences if not promptly treated. Common causes of intracranial hemorrhages include hypertension (high blood pressure), stroke, and traumatic brain injury [5, 6].

Hemorrhaging within the brain can occur in two primary locations: either within the confines of the skull but outside the brain or within the brain tissue itself. Between the skull and brain tissue, there are three protective membrane layers known as meninges. These layers comprise the outermost dura mater and the middle arachnoid, and the innermost pia mater, which rests directly against the brain. Bleeding can occur anywhere between the three meninges. Based on lesion location in the brain, Intracranial hemorrhagic (ICH) is divided into five subtypes shown in Fig 1.3. Subarachnoid hemorrhage (SAH), subdural hemorrhage (SDH), and epidural hemorrhage (EDH) all fall under the category of intracranial hemorrhage. that occur outside the brain but inside the skull. intraventricular hemorrhage (IVH) and intraparenchymal hemorrhage (IPH), These two types of intracranial hemorrhage can occur inside the brain tissue itself. Intracranial hemorrhagic is significantly more dangerous and challenging to treat, underscoring the importance of a thorough analysis of hemorrhagic images in medicine. These distinct types of intracranial hemorrhage present varying challenges in terms of diagnosis and treatment. Subarachnoid hemorrhage, occurring in the space between the brain and the surrounding membranes, often results from ruptured aneurysms and demands prompt medical attention. Subdural hemorrhage involves bleeding in the space between the brain and its outer covering, typically due to head trauma. Epidural hemorrhage, caused by arterial bleeding between the skull and outermost brain membrane, is often associated with head injuries. On the other hand, intraventricular hemorrhage and intraparenchymal hemorrhage, both occurring within the brain tissue, can be caused by various factors, including hypertension or vascular abnormalities. These intracranial hemorrhages within the brain pose

intricate challenges due to their potential impact on vital brain structures and functions.[5–7].

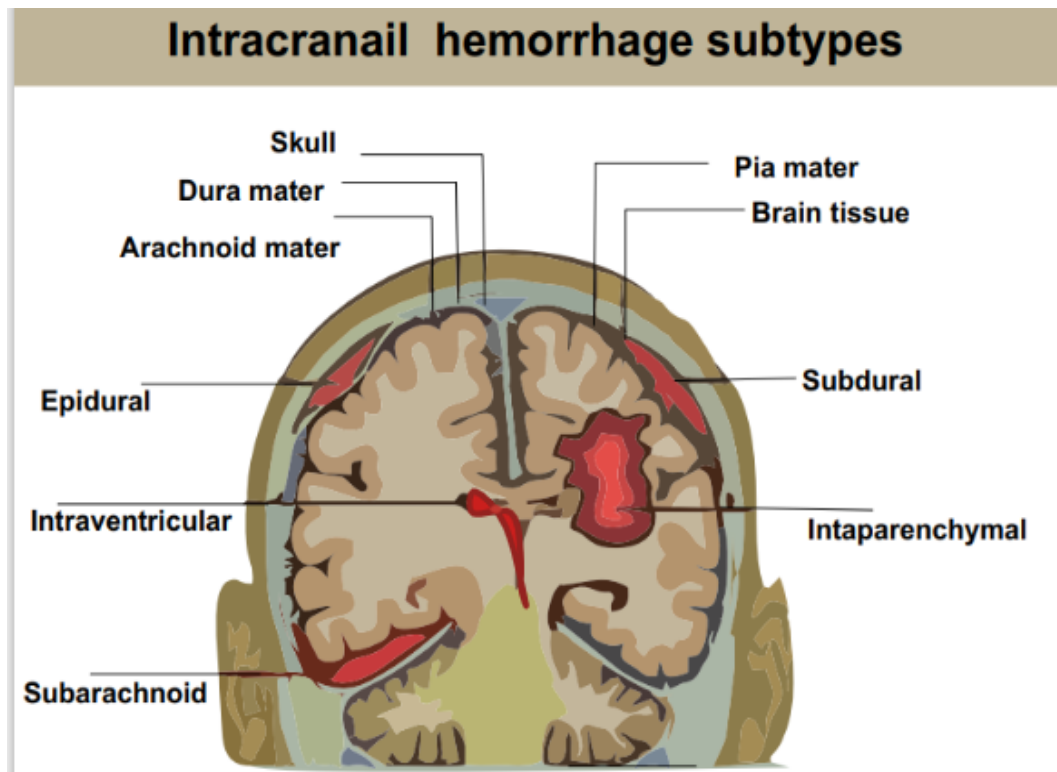


FIGURE 1.3: Subtypes of Intracranial Hemorrhage

#### 1.1.1.1 Subarachnoid Hemorrhage

A Subarachnoid Hemorrhage (SAH) is a type of bleeding within the skull but outside the brain tissue, occurring between the dura mater and the arachnoid mater—two middle layers. This condition arises when a blood vessel on the brain's surface ruptures, often triggered by head trauma. The resulting blood accumulation around the brain and inside the skull exerts pressure on the brain, leading to potential damage to brain cells, persistent issues, and challenges in daily life. A sudden and intense headache is the primary symptom, with some individuals describing it as the most severe headache they have ever encountered. Prompt medical attention is crucial for diagnosing and managing SAH to mitigate its consequences effectively. Recovery from SAH can be complex and may involve rehabilitation efforts to address cognitive and physical impairments. Long-term outcomes depend on various factors, including the extent of the hemorrhage, the

effectiveness of interventions, and individual health conditions. This underscores the importance of a comprehensive and multidisciplinary approach in managing patients with SAH to optimize their recovery and long-term well-being.[5–8].

#### **1.1.1.2 Subdural Hemorrhage**

Subdural hemorrhage(SDH) transpires as a consequence of blood vessel rupture between the brain and the dura mater, causing bleeding within the gap between the brain and the skull. Subdural hemorrhage is a common complication of head injuries, occurring in up to 25% of cases. The symptoms of subdural hemorrhage are caused by the increased pressure that the blood clot exerts on the brain. This pressure makes it difficult for the neurons in the brain to function properly, leading to a variety of symptoms. This category of hemorrhage can be induced by not only head trauma but also blood clotting disorders and brain tumors[5–8].

#### **1.1.1.3 Epidural Hemorrhage**

Epidural hemorrhage (EDH) is a form of brain bleeding situated between the skull and the dura mater, which is the outermost layer of the meninges. This condition is often the result of a head injury that damages an artery. Symptoms associated with EDH can vary depending on the size and location of the bleed, but typically encompass a sudden and severe headache, loss of consciousness, and potential seizures. Some instances may involve a brief period of alertness following the injury, followed by a rapid deterioration in the patient's condition. EDH is considered a medical emergency, necessitating immediate treatment[5–8].

#### **1.1.1.4 Intraparenchymal Hemorrhage**

Intraparenchymal hemorrhage (IPH) is a condition that arises when a blood vessel inside the brain ruptures, resulting in internal bleeding within the brain's tissue. This bleeding occurs within the brain's parenchyma. Various factors can trigger IPH, such as high blood pressure, aneurysms, arteriovenous malformations

(AVMs), and head injuries. Symptoms of IPH can vary based on the size and location of the bleed but often encompass a sudden and intense headache, vomiting, seizures, and weakness or paralysis on one side of the body. IPH is deemed a medical emergency, necessitating immediate treatment[5–8].

#### 1.1.1.5 Intraventricular Hemorrhage

Intraventricular hemorrhage (IVH) is a specific type of brain bleed that occurs within the ventricles, which are fluid-filled cavities within the brain. Although IVH is the rarest form of stroke, its potential severity demands attention. This condition arises from the rupture of a blood vessel within the brain and can be triggered by several factors. Among the causes, high blood pressure stands as the most prevalent contributor to IVH. Aneurysms, weakened spots in blood vessels that can rupture and lead to bleeding, also constitute a significant causative factor. Similarly, arteriovenous malformations (AVMs), tangled blood vessel clusters that are prone to rupturing, can induce IVH. Traumatic incidents, such as head injuries, can trigger brain bleeding, as can cocaine use, which elevates the risk of IVH. Even traumatic brain injuries can precipitate brain hemorrhaging[5–8].

## 1.2 Computer-Aided Diagnosis(CAD) System for Intracranial Hemorrhage Classification

Identifying the type of intracranial hemorrhage is essential for medical professionals to provide the best possible care for the patient. The kind of hemorrhage will determine the course of treatment, including medications, surgery, and rehabilitation. Each subtype offers distinct insights into the underlying pathology and potential causative factors, aiding doctors in formulating targeted treatment strategies. For instance, understanding whether a patient has suffered an intraparenchymal hemorrhage, which originates within brain tissue, compared to subarachnoid bleeding caused by ruptured vessels between meningeal layers, informs differential interventions. This knowledge influences decisions about the necessity

of surgical procedures, the administration of specific medications, or the monitoring of certain complications[9, 10].

Prompt and precise identification of intracranial hemorrhage via medical imaging plays a critical role in delivering timely medical interventions. This timely response significantly enhances patient outcomes and prognosis[8, 11]. Conventional approaches for visualizing brain lesions involve the use of computed tomography (CT) and magnetic resonance imaging (MRI). In evaluating stroke patients, the recommended initial approach is a CT scan. This is because CT scans have demonstrated effectiveness in swiftly assessing whether an individual is undergoing a stroke. CT scans can identify hemorrhage strokes with more than 92% accuracy. The automated identification of sub-type of intracranial hemorrhage (ICH) from CT scan images has become a significant concern within both the Deep learning and medical domains[11].

Additionally, recognizing the type of intracranial hemorrhage guides doctors in predicting the patient's recovery trajectory and potential long-term consequences. It enables them to provide patients and their families with accurate prognostic information, thereby fostering informed decision-making. The precision in diagnosis also serves as a cornerstone for ongoing research efforts, contributing to the advancement of medical knowledge, refining diagnostic tools, and enhancing therapeutic approaches in the realm of neurology. CAD systems play a crucial role in mitigating human errors and delivering swift, precise quantitative, and qualitative evaluations of Intracranial Hemorrhage (ICH) as indicated by references. This technological progression presents a transformative potential for significantly improving clinical outcomes. Traditional Computer-Aided Diagnosis (CAD) systems primarily focus on reducing false negatives by identifying unique features crucial for clinicians in spotting irregularities. The evolution of CAD systems through ongoing research has expanded their functionalities, enabling diverse image analysis techniques for disease detection, treatment planning, risk prediction, and prognosis assessment. Radiologists can utilize CAD system interpretations as supplemental tools to inform their final diagnostic decisions[12]. Modern CAD systems, incorporating machine learning and deep learning methodologies, exhibit the capability

to rapidly assimilate and predict anomalies within extensive datasets. Numerous methodologies have been introduced to diagnose brain irregularities in images, representing diverse modalities. These approaches operate in semi-automated or fully automated modes, facilitating the detection of singular or multiple brain abnormalities. Additionally, they offer both supervised and unsupervised functionalities, enhancing their versatility and applicability in various clinical scenarios. This paradigm shift in medical imaging analysis holds great promise for more accurate and efficient diagnosis, contributing to enhanced patient care and treatment planning.[13–15].

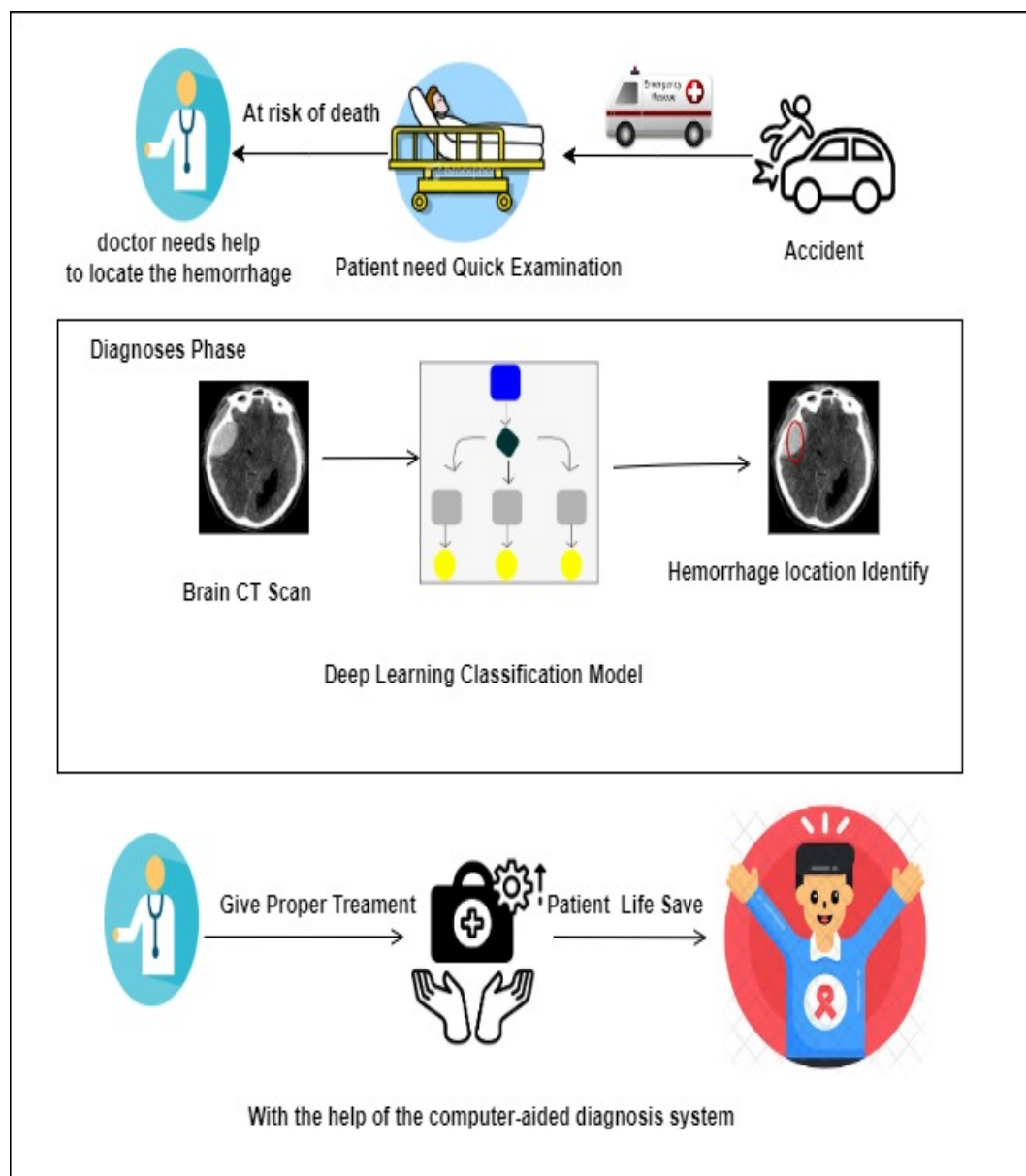


FIGURE 1.4: Brain Hemorrhage Classification using Computer-Aided Diagnosis System



### 1.3 Methods Used for Intracranial Hemorrhage Classification.

Computer-aided diagnosis (CAD) is a prevalent tool employed in clinical settings to facilitate the early identification and diagnosis of irregularities within medical images. CAD systems play a crucial role in assisting radiologists by enhancing the precision and uniformity of their evaluations concerning the detection and classification of intracranial hemorrhages. By furnishing supplementary information, CAD systems empower clinicians to formulate more precise prognoses and clinical judgments. Furthermore, these systems contribute to the reduction of human errors and offer expeditious, cost-effective, and comprehensive quantitative and qualitative appraisals of intracranial hemorrhages, thereby benefiting the overall diagnostic process[12].

Computer-Aided Diagnosis (CAD) systems specializing in Intracranial Classification are sophisticated software applications developed to aid healthcare professionals in precisely categorizing and detecting abnormalities or conditions within the cranial region. Tailored for the interpretation of medical images, such as brain CT scans or MRIs, these systems play a pivotal role in enhancing the diagnostic process. Their overarching objectives include improving diagnostic accuracy and providing supplementary insights into a spectrum of intracranial conditions, spanning from hemorrhages and tumors to various neurological disorders. The integration of CAD systems in the medical field underscores their potential to contribute significantly to diagnostic efficiency and precision in the realm of intracranial health assessment. The primary goal of CAD systems for Intracranial Classification is to enhance the diagnostic process, improve accuracy, and provide additional insights into various intracranial conditions, including hemorrhages, tumors, or neurological disorders. These CAD systems operate by employing advanced algorithms and machine learning techniques to analyze complex patterns and features within medical images. By automating the detection and classification processes, they assist healthcare professionals in making more informed decisions during diagnosis. Additionally, CAD systems contribute to streamlining

the workflow in medical imaging, allowing for quicker assessments and potentially reducing the chances of oversight[13, 14].

Intracranial Classification CAD systems are particularly valuable in identifying subtle or early signs of conditions such as hemorrhages, where prompt and accurate diagnosis is critical. Their ability to handle large datasets and detect nuanced patterns makes them powerful tools in the evolving landscape of medical imaging and diagnostics. The integration of such systems showcases the synergy between technological advancements and healthcare, aiming to enhance patient outcomes and facilitate more efficient clinical practices[13, 14]. Two primary methods employed in the classification of intracranial hemorrhage are:

### 1. **Feature Learning-Based Approach:**

Feature learning-based techniques are at the core of Computer-Aided Diagnosis (CAD) systems for medical image analysis, including the classification of intracranial hemorrhage (ICH). These techniques are designed to automatically discover relevant patterns and discriminative features within medical images, allowing for accurate disease detection and classification. A standard feature learning-based CAD system comprises several key stages, including preprocessing, feature extraction, dimensionality reduction, and classification [16]. Preprocessing plays a pivotal role in enhancing the performance of Intracranial Hemorrhage detection and Classification. Pre-processing techniques, such as noise reduction and artifact removal, are systematically applied to CT images to enhance their overall quality and prepare them for subsequent analysis [17]. The process of identifying intracranial hemorrhages (ICH) from CT images relies significantly on feature extraction, a crucial step aimed at revealing intricate patterns inherent in the images. Visual inspection alone can be challenging for this task, emphasizing the need for systematic feature extraction methods to ensure accurate and efficient analysis. In this context, dimensionality reduction plays a pivotal role by assisting in the selection of the most relevant features from the complex dataset. This strategic reduction in dimensionality not only aids in enhancing computational efficiency but also contributes to the identification of critical patterns

and features essential for accurate diagnosis and classification of intracranial hemorrhages [18], allowing for the characterization of the diverse injuries associated with ICH sub-classes. These reduced features are then used by various classifiers to identify the presence and severity of ICH sub-classes. Subsequent sections provide a detailed breakdown of the stages within CAD systems. Figure 1.5 is an illustration of a typical feature learning-based approach[16–18].

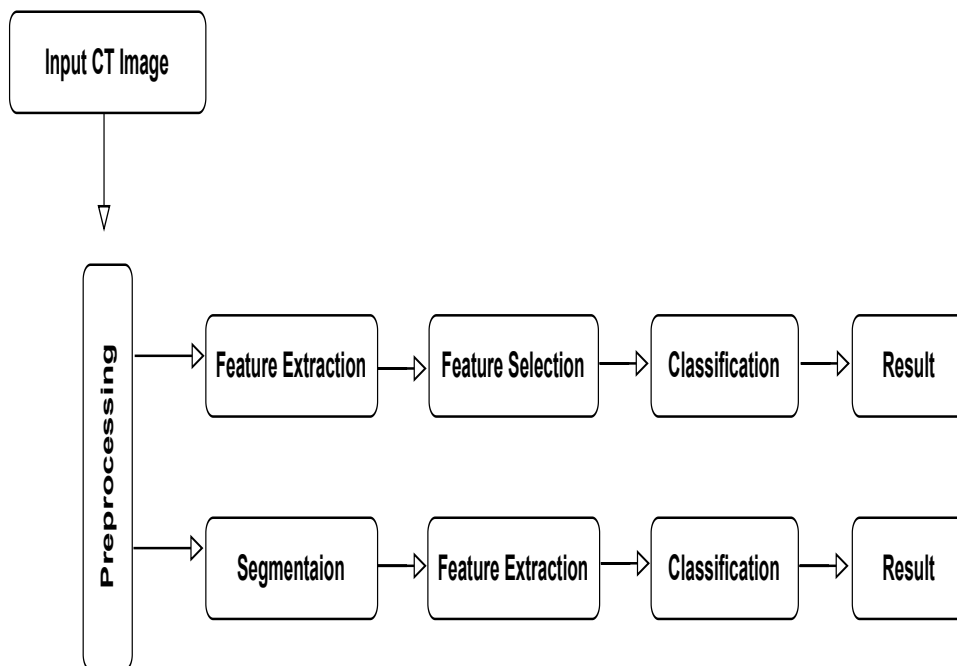


FIGURE 1.5: Schema of Feature Learning-Based Method for Intracranial Hemorrhage (ICH).

## 2. Deep Learning-Based Approach:

Deep learning has brought about a transformative impact on the realm of medical image analysis, encompassing tasks like identifying and categorizing intracranial hemorrhage (ICH). Deep learning methodologies, powered by artificial neural networks with multiple hidden layers, empower CAD systems to autonomously glean intricate patterns and features directly from medical images. This paradigm shift in image analysis not only enhances the accuracy of detection but also allows for a more comprehensive understanding of complex medical conditions, contributing to more effective diagnostic processes in the field of healthcare. The utilization of artificial neural

networks, characterized by multiple hidden layers, enables these systems to autonomously extract intricate patterns and features directly from medical images, particularly in tasks involving the identification and categorization of intracranial hemorrhage (ICH). The automated learning process not only improves the accuracy of detection but also enhances the overall efficiency of diagnosis, offering healthcare professionals valuable insights into complex medical conditions. This transformative impact underscores the potential of deep learning to revolutionize and elevate the field of medical imaging and diagnostic practices.

Convolutional Neural Networks (CNNs) have emerged as pivotal tools within biomedical domains, leveraging their innate capacities for self-organization and autonomous learning. These networks have proven to be particularly adept at extracting intricate patterns and features from complex biomedical data, making them invaluable in tasks such as medical image analysis and classification. The ability of CNNs to discern hierarchical representations within data sets contributes to their success in various applications, enhancing the efficiency and accuracy of tasks related to healthcare, diagnostics, and biomedical research. As a result, CNNs continue to play a significant role in advancing the capabilities of computational models in the biomedical field. As illustrated in Figure 1.6. The architecture of a Convolutional Neural Network (CNN) comprises a sequential arrangement of convolutional and pooling layers, strategically organized to cater to a diverse range of applications. This design allows CNNs to effectively capture hierarchical features and spatial information from input data, making them well-suited for tasks such as image recognition, classification, and segmentation. The convolutional layers enable the network to detect local patterns, while pooling layers assist in reducing spatial dimensions, enhancing the network's ability to recognize and learn from complex patterns within the data. This inherent structure makes CNNs versatile and powerful for various applications in the field of deep learning and image processing. [19]. The convolutional layers utilize predetermined-sized convolutional to capture features. Then consolidated and spatially reduced through a pooling layer, which employs

methods like max pooling or average pooling [19, 20]. Following this, the extracted features traverse through fully connected layers, ultimately reaching the network's output units[21, 22].

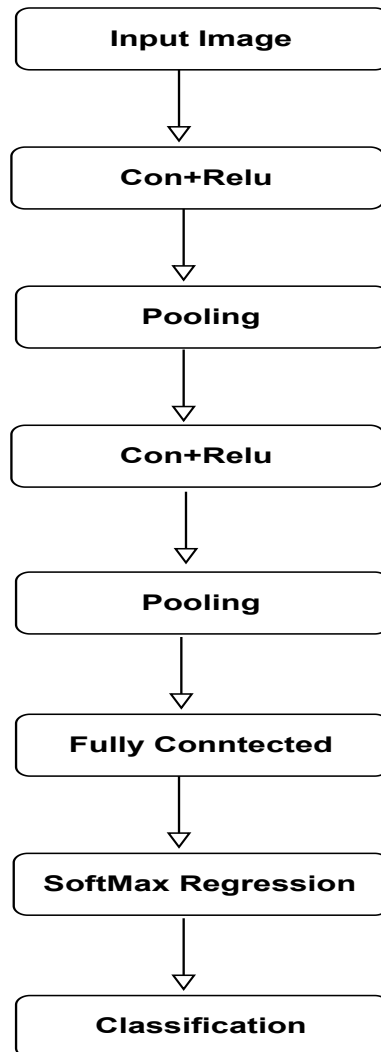


FIGURE 1.6: A Deep Learning Model Structure for Intracranial Hemorrhage Classification

## 1.4 Motivation

In recent years, medical imaging has emerged as a pivotal field for diagnosing and monitoring various health conditions, providing invaluable insights into internal structures and anomalies that might otherwise go unnoticed. The concept of computer-based clinical decision support has been increasingly popular as a research topic to improve the quality of decision-making in the field of medicine and

healthcare domain. Intracranial hemorrhage, a critical condition characterized by bleeding within the brain, demands prompt and accurate diagnosis to mitigate potentially severe consequences. With the advancement of medical imaging technologies, the promise of automating the detection and classification of intracranial hemorrhages using deep learning models has grown significantly. Traditional diagnosis can vary among doctors and in different situations. Nevertheless, this approach faces challenges related to low image contrast and the complex appearance of lesions. The need for accurate intracranial hemorrhage (ICH) classification arises from its critical implications for patient well-being, medical decision-making, and healthcare efficiency[10, 23]. Central to this pursuit is the RSNA (Radiological Society of North America) Intracranial Hemorrhage dataset, a notable contribution in this domain. Curated with meticulous care by domain experts, this dataset encompasses a diverse array of brain imaging scans, meticulously annotated to indicate the presence or absence of various classes of intracranial hemorrhages. Encompassing a wide spectrum of cases and imaging modalities, this dataset provides a solid groundwork for the development and assessment of classification models[24].

## 1.5 Problem Statement

The classification of intracranial hemorrhage (ICH) through the analysis of computed tomography (CT) images plays a critical role in accurately diagnosing hemorrhagic conditions in emergency departments [23]. The accurate and timely detection of intracranial hemorrhage is critical for patient prognosis and treatment. Timely intervention can help prevent further bleeding, minimize neurological damage, and improve patient outcomes [9]. Existing auxiliary diagnosis algorithms give equal weight to each location's characteristics. The model's trained features for classification contain noise or features without any diagnostic value, which significantly reduces system performance and reliability. The accuracy of detecting intracranial hemorrhage hinges significantly on the precision of lesion segmentation, a task known for its complexity. Leveraging deep learning models holds the potential to enhance this accuracy by extracting precise features. This, in turn,

facilitates the automation of the classification process, leading to quicker and more efficient diagnoses, ultimately benefiting patient care.

## 1.6 Significant of the Solution

This study proposes a new approach for classifying intracranial hemorrhages using an attention U-Net model. The goal is to develop a method that is both accurate and efficient, and that uses all available information in the medical images. The attention U-Net is a deep learning model that is known for its ability to capture intricate spatial patterns. It does this by using an attention mechanism, which allows the model to dynamically focus on different regions of interest within the image. This ensures that the most important features of the hemorrhage are highlighted, which improves the accuracy of classification[25]. The proposed approach addresses the challenge of accurately detecting intracranial hemorrhages, which can have a complex and variable appearance. Traditional models often struggle to account for these variations, leading to inaccurate classifications. However, the attention U-Net is able to dynamically refine its understanding of the hemorrhage features, resulting in more robust and precise classifications. This innovative approach has the potential to advance the field of automated intracranial hemorrhage diagnosis. Integrating attention mechanisms into the U-Net framework represents a state-of-the-art technique with the potential to attain elevated classification accuracy. Such advancements have the capacity to enhance patient care and elevate the standards of medical diagnostic procedures.

## 1.7 Research Questions

1. How can interpretability deep learning models be improved for Classification different type of intracranial Hemorrhage?
2. How can the class imbalance issue in intracranial hemorrhage datasets be effectively addressed to improve the performance of classification models?

3. Can the Attention U-Net model be used to extract and utilize distinctive features to enhance its performance in classifying various intracranial hemorrhage subtypes?

## 1.8 Thesis Organization

In this thesis chapters are structured as follows: Chapter 1 introduces the Intracranial Hemorrhage and its Sub-classification which consists of subdivisions like motivation and problem statement of proposed work. Chapter 2 conducts a comprehensive literature review of segmentation and classification models for Intracranial Hemorrhage. It delves into the established techniques for image pre-processing, feature extraction, segmentation, feature selection, and the subsequent classification. Chapter 3 outlines the methodology employed in this study, focusing on the utilization of the Attention UNET Model to extract deep features. Chapter 4 presents the results and engages in a thorough discussion of the findings. Lastly, Chapter 5 encapsulates the conclusions drawn from the study's outcomes.



# Chapter 2

## Literature Review

Advances in image processing have led to a growing interest in the detection of intracranial hemorrhages in recent decades. Researchers are using various detection and classification techniques to identify and classify hemorrhages.

### 2.1 Survey of Existing Techniques

The fundamental stages involved in the identification and classification of intracranial hemorrhages encompass pre-processing, segmentation, feature extraction, and classification.

Preprocessing serves as an essential technique to enhance poorly illuminated images, serving as a preliminary step prior to analysis [26]. Its primary goal is to refine image data and eliminate noise, thereby improving visualization. Preprocessing encompasses a range of techniques, including edge detection, color transformation, image filtering, contrast enhancement, scaling, brightness correction, and geometric transformation [27]. To enhance the quality of DICOM Images, various preprocessing techniques such as windowing, resizing, Normalization and zero-centering techniques are applied, particularly using Hounsfield Units (HU) play a vital role in CT scans by quantifying the densities of objects based on the absorption of X-rays. An object's density is determined by the amount of X-rays

it absorbs, with HU values typically ranging from -1000 to +1000. Lower HU values signify higher X-ray absorption and lower density, while higher values indicate lower absorption and higher density[23, 28]. Radiologists frequently modify window settings when interpreting brain CT scans to emphasize various intensity ranges for detecting subtle abnormalities. For instance, they commonly employ the brain window with settings at a window level of 40 and width of 80, as well as the subdural window with a level of 80 and width of 200[26]. These adjustments enhance the visibility of intracranial hemorrhages, aiding in the detection of thin acute subdural hematomas that might otherwise go unnoticed. Furthermore, the bone window, configured with a level of 600 and width of 2800, is essential for identifying lesions in the skull[27]. Resizing is crucial to ensure that images are of uniform dimensions, making them compatible with the neural network architecture. It helps streamline the data for processing and ensures that the model can handle inputs of the same size, which is essential for training and inference[19, 29, 30]. In the context of existing studies on hematoma region detection, various supervised classifiers have been widely used. These classifiers include Support Vector Machine (SVM), Random Forest (RF) featured, Artificial Neural Network (ANN), Probabilistic Neural Network (PNN), Bayesian, Multinomial Logistic Regression, and Tree Bagger classifiers. Recently, deep Convolutional Neural Networks (CNNs) have demonstrated remarkable generalization capabilities, owing to their ability to self-learn and self-organize without explicit programming. In 2018, Grewal et al. introduced a model named Recurrent Attention DenseNet (RADnet), which incorporated a bi-directional long short-term memory (Bi-LSTM) layer with DenseNet for the diagnosis of hemorrhages. Their model exhibited notable performance, achieving an accuracy of 81.82%, sensitivity of 88.64%, and precision of 81.25% in predicting hemorrhages. These results were comparable to the diagnostic capabilities of radiologists when applied to CT scans. Their study was conducted using a dataset consisting of 77 brain CT scans, and the Bi-LSTM layer was integrated to capture dependencies across slices within the scans. However, the paper did not address the classification of intracranial hemorrhage subtypes [29]. In the same year, Arbabshirani et al. introduced a deep learning-based method for the detection of intracranial hemorrhage (ICH) in head computed tomography (CT)

scans. Their approach utilized a convolutional neural network (CNN) trained on a sizable dataset consisting of both CT scans with and without ICH. The CNN effectively learned spatial features associated with ICH, enabling it to accurately identify ICH in previously unseen scans. Their method underwent evaluation using a dataset comprising 9499 CT scans, resulting in a commendable accuracy rate of 92.5% for ICH detection. Furthermore, in a clinical context, the approach demonstrated a remarkable 96% reduction in the time required for ICH diagnosis, showcasing its potential for real-world applications [30]. In 2019, Cho et al. comprised two convolutional neural networks (CNNs) and dual fully convolutional networks (FCNs). The cascade CNN is dedicated to identifying bleeding, while the dual FCN is designed to detect and delineate five subtypes of intracranial hemorrhage. The model was trained on a substantial dataset of CT images with two different window settings. Combining these settings resulted in a notable improvement in sensitivity (97.91%) without compromising specificity (98.76%) for binary classification. Additionally, the segmentation of bleeding lesions demonstrated an overall precision of 80.1% and recall of 82.15%, marking a 3.44% enhancement compared to using a single FCN model[31]. In 2019, Ye et al. proposed a novel 3D joint convolutional and recurrent neural network (CNN-RNN) that was used for detecting intracranial hemorrhage (ICH) and its five subtypes in non-contrast head CT scans. The research involved 2836 subjects and 76,621 CT slices from three institutions. CNN-RN framework performed remarkably well, achieving excellent metrics for binary (bleeding or not) algorithm achieved  $>0.98$  AUC and multi-class (five subtypes) classifications algorithm achieved  $>0.8$  AUC [32]. In 2019 Bar et al. introduced BloodNet, a deep-learning model designed to enhance the triaging of Head CT scans, particularly for the timely detection of Intracranial hemorrhage (ICH) in emergency settings. BloodNet optimizes the segmentation and classification tasks by incorporating their dependencies, resulting in improved classification outcomes. The model achieved impressive AUCs of 0.9493 and 0.9566 in different datasets containing over 1400 studies from various hospitals. These results are on par with previous findings, even with a larger dataset, demonstrating the potential for faster and more accurate ICH detection using this approach[33]. In 2019, Dawud and colleagues employed deep learning techniques to distinguish

between brain CT images depicting hemorrhage and those that did not. They developed and trained three distinct models for this task: a convolutional neural network (CNN), the renowned AlexNet neural network, and a customized variation of AlexNet combined with a support vector machine (SVM) classifier. Remarkably, the AlexNet-SVM model outperformed the others, achieving an impressive accuracy of 93%, with a sensitivity of 90% and specificity of 95%. However, it's worth noting that this study did not address the classification of specific subtypes of intracranial hemorrhage[19]. In 2020, He et al. employed deep convolutional neural networks, specifically SE-ResNeXt50 and EfficientNet-B3, to extract features from head CT scans and classify five subtypes of intracranial hemorrhage. Their dataset was sourced from the Radiological Society of North America via a Kaggle competition. The findings demonstrate that an ensemble of these networks, trained using weighted multi-label logarithmic loss, achieved an exceptional level of accuracy in intracranial hemorrhage classification, comparable to expert-level performance[34]. Guo et al. (2020) have presented a deep learning-driven approach for the concurrent classification and segmentation of intracranial hemorrhage (ICH) in brain CT images. The method leverages a fully convolutional neural network (FCN) that is designed to generate both a segmentation map and a classification label for each pixel within the CT image. The FCN comprises a sequence of convolutional layers responsible for feature extraction from the CT image and subsequent upsampling layers that restore the image to its original resolution. The FCN's output includes a segmentation map, which provides the probability of each pixel being classified as hemorrhagic or non-hemorrhagic. The classification label is determined based on the highest probability value within the segmentation map. The study evaluated the method using a dataset containing 1176 CT images featuring ICH. The reported results indicated a detection accuracy of 92.9% and a segmentation Dice score of 0.86, highlighting the model's effectiveness in both identifying and delineating intracranial hemorrhages[35]. Hssayeni et al. (2020) introduced a deep learning-based approach for the identification and delineation of intracranial hemorrhage (ICH) in computed tomography (CT) images, comprising two key stages: detection and segmentation. In the detection stage, a convolutional neural network (CNN) is employed to categorize each pixel within the CT

image as either representing a healthy or hemorrhagic region. In contrast, the segmentation stage utilizes a U-Net-based CNN to precisely delineate the areas of hemorrhage in the CT image. The method was rigorously evaluated on a dataset comprising 82 CT images that had been annotated by two radiologists to identify ICH. The outcomes demonstrated the effectiveness of the approach, achieving a detection accuracy of 93.8% and a segmentation Dice score of 0.8. These results underscore the model's proficiency in both detecting and precisely segmenting intracranial hemorrhages[36].

In 2020, Mantas et al. presented a model, based on ResNexT architecture, that was tested on actual CT scans from patients at N.N. Burdenko Neurosurgery Center. Impressively, the model achieved a detection accuracy exceeding 0.81 for all hemorrhage subtypes without requiring any further tuning[37]. In Ko et al.'s (2020) study, they developed a deep learning model for predicting the presence of intracranial hemorrhage (ICH) in single-head computed tomography (CT) scans. The model was trained on a substantial dataset of 4,516,842 head CT scans, which were processed to create three different images with specific windows: brain window, bone window, and subdural window. Their model employed a deep convolutional neural network (CNN) based on the Xception architecture, coupled with a long short-term memory (LSTM) network featuring 64 nodes and 32 timesteps. Remarkably, the model achieved a remarkable accuracy rate of 93.8% for identifying ICH and 86.2% for classifying the specific type of ICH[38].

In 2021 Raghavendra et al. presents a computer-aided diagnosis model that uses image processing and probabilistic neural networks with CT images to detect intracerebral hemorrhage. The model achieved an impressive 97.37% accuracy in distinguishing normal from hemorrhagic cases[28]. Mansour et al.(2021) have introduced a deep learning-driven approach for the segmentation of intracranial hemorrhage (ICH) in brain CT images. Their method relies on a convolutional neural network (CNN) constructed upon the Inception architecture. The dataset utilized for training and evaluation included 3725 head CT images containing instances of ICH. These images were sourced from two publicly accessible datasets: the MICCAI ICH Stroke Repository and the INRIA-STROKE dataset. The reported

results indicated that the method achieved a Dice score of 0.86, which measures the degree of overlap between the predicted and ground truth segmentation. However, the paper did not include any classification results for distinguishing between different types of ICH[39]. In 2021 Watanabe et al. assessed the impact of deep learning-based computer-assisted detection (CAD) on the performance of physicians with varying levels of expertise in detecting intracranial hemorrhage using CT scans. A total of 40 head CT datasets were reviewed by 15 physicians, including board-certified radiologists, radiology residents, and medical interns, during two reading sessions with and without CAD. The CAD system, developed using 433 patient CT images, provided probability heat maps for hemorrhage regions. The results showed that CAD significantly improved overall accuracy, with mean accuracy rising from 83.7% to 89.7%. Board-certified radiologists benefited the most from CAD, achieving an accuracy of 97.5 % [40]. In 2021 Zhang et al. proposed a novel approach is presented, involving the synthesis of artificial ICH lesions on non-lesion CT images. This is achieved through the Artificial Mask Generator (AMG) for creating masks and the Lesion Synthesis Network (LSN) for converting them into hemorrhage lesions. These augmented images, containing both real and synthetic lesions, are used to train an ICH detection model with a Residual Score. Experimental results show a significant enhancement in ICH detection, classification, and improved sensitivity for microbleeding, surpassing other synthetic approaches. The proposed method boosts the AUC value from 84% to 91% for ICH detection and from 89% to 96% for classification, making it a promising advancement in CAD for ICH diagnosis[41].

In 2022, Kumar et al. introduced an automated and unsupervised approach for segmenting intracranial hemorrhages in CT images based on entropy. This method combines several techniques, including fuzzy c-mean (FCM) clustering, automatic cluster selection, skull removal, thresholding, and edge-based active contour methods. FCM is initially employed to partition the image into clusters, with one cluster automatically chosen to focus on the skull and hemorrhage regions. The experiment was conducted using 35 CT images from different patients. The results indicate that the proposed method yields highly accurate hemorrhage region

segmentation when compared to both FCM and manual fuzzy-based active contour methods[42]. In 2022 Anupama et al. present a novel approach, the GC-SDL model, for diagnosing intracerebral hemorrhage (ICH) using deep learning and GrabCut-based segmentation. It addresses the challenge of time-consuming manual CT scan segmentation by employing Gabor filtering for noise reduction and GrabCut-based segmentation for effective identification of diseased areas. The synergic deep learning (SDL) model is then used for feature extraction, with a softmax (SM) layer serving as the classifier. Extensive experiments on a benchmark ICH dataset reveal the GC-SDL model's impressive performance, boasting a sensitivity of 94.01%, specificity of 97.78%, precision of 95.79%, and an overall accuracy of 95.73%[43]. Ganeshkumar et al. (2022) have presented a deep-learning approach for the identification and segmentation of intracranial hemorrhage (ICH) in brain CT images. Their method comprises two stages: identification and segmentation. In the identification stage, ResNet, a convolutional neural network (CNN), is employed to classify each voxel in the CT image into ICH subtypes. For segmentation, SegAN is utilized to delineate hemorrhagic regions within the CT image. To tackle class imbalance in the ICH dataset, the authors incorporate the data augmentation technique CycleGAN. The dataset employed in this study is publicly accessible on PhysioNet. The method demonstrated a detection accuracy of 0.85% for ICH and achieved a segmentation Dice score of 0.32. It's important to note that this method does not differentiate between different subtypes of intracranial hemorrhage (ICH)[44]. In 2022 Zhang et al. presented a weakly supervised guided soft Attention network for the classification of intracranial Hemorrhage. First extract the multi-scale feature of the CT scan using the MSFE module then the weak knowledge extraction module, used to process data and obtain the weak knowledge, which is used to guide the attention module. Attention module to learn features from segmentation annotations then classify the image into six categories. This network achieved 98.1 % accuracy, 68.4 % TPR rate, and 74.6 % f1 score [9].

In 2023 Nizarudeen et al. produced an innovative approach for the Detection and Categorization of Acute Intracranial Hemorrhage (ICH) subtypes using a Multi-Layer DenseNet-ResNet Architecture with an Improved Random Forest Classifier

(IRF). The goal is to enhance the accuracy and reduce computational time in identifying ICH subtypes from brain CT images. The proposed method utilizes a combination of DenseNet and ResNet architectures for feature extraction, followed by classification using the Improved Random Forest (IRF) Classifier. The results demonstrate significantly higher accuracy compared to existing approaches, making it a promising technique for more precise and efficient ICH diagnosis[45].

In 2023 Cortes et al. Introduced a novel approach utilizing EfficientDet’s deep-learning technology to diagnose hemorrhages at the patient level, potentially serving as a decision support system. The method can classify computed tomography scan slices to determine the presence or absence of hemorrhage, achieving an impressive 92.7% accuracy and 0.978 ROC AUC for patient-level diagnosis[46].

In 2023 Arman et al. proposed an automated method for diagnosing intracranial hemorrhage from CT scans. The DenseNet architecture was optimized using Bayesian Optimization (BO) to enhance effectiveness. BO determined the optimal learning rate, optimizer, and number of dense nodes. The optimized DenseNet model achieved an impressive 98.02% accuracy on the test set. This approach ensures precise diagnoses, aiding doctors in making informed decisions and providing better patient care[47].

TABLE 2.1: Analysis of Existing Techniques

Reference	CT Dataset	Method	Remarks
[29]	392 Annotated	REDNET	Only have Binary Classification
[30]	46583	CNN Model	Only have Binary Classification
[31]	135974	CNN and Dual FCN	Only have Binary Classification
[32]	2836 Annotated	Combine CNN,RNN Model	Only have Four type Classification
[33]	175 Annotated	BloodNet	Sub Classification Result Not Found.



[34]	RSNA Intracranial Hemorrhage	19	SE-Resnet50, EfficientNet-B3	Sub Classification Result not Found
[19]	Images collected from the Aminu Kano Teaching Hospital, Nige- ria		CNN, AlexNet-SVM	Only have Binary Classification
[35]	1176		ICHNet Architecture	Five type Classi- fication ,Avg F1 score (0.561)
[36]	82 Annotated		UNET	Only Segmentation Performed
[37]	RSNA Intracranial Hemorrhage	19	ResNet Architecture	Achieved accuracy of 80% on each Class.
[38]	RSNA Intracranial Hemorrhage	19	CNN-LSTM Model	Only have Binary Classification
[28]	1603		Non Linear Feature Extrac- tion,KNN+PNN+SVM	Only have Binary Classification
[39]	3725		Kapurs Multilevel Thresh- olding,CNN Base Inception V4	0.86 Dice Score But No classification Result
[40]	40 Annotated		UNET	Accuracy(97.5) % but Each Class Ac- curacy Not Given
[43]	82 Annotated		GC-SDL	Only Segmentation but No classifica- tion Result

---

[42]	35		Fuzzy C Mean Cluster, Automatic Cluster Selection edge base Method	Only Segmentation but No classification Result
[44]	82 Annotated		ResNet,SegAN	0.32 Dice Score
[45]	82 Annotated		ResNet-DenseNet-XGBoost Classifier	Acc (0.92)
[9]	RSNA	19	MSFE, WGSJ JFM	Avg F1(0.74)
	Intracranial Hemorrhage			
[45]	82 Annotated		ResNet-DenseNet-XGBoost Classifier	Acc (0.92)
[46]	RSNA	19	Grad-CAM methodology	92.7% Accuracy
	Intracranial Hemorrhage			
[47]	RSNA	19	DenseNet architecture optimized using Bayesian Optimization	Avg F1(0.78)
	Intracranial Hemorrhage			

---

## 2.2 Research Gap

The classification of intracranial hemorrhage (ICH) using computed tomography (CT) images are important for the proper diagnosis of hemorrhage in emergency departments with acceptable accuracy. To address this issue, it is required to generate a deep learning model that can extract the feature precisely for better classification of different types of neurological diagnoses. Existing auxiliary diagnosis algorithms give equal weight to each location's characteristics and place no restrictions on newly learned features. The model's trained features for classification contain noise or features without any diagnostic value, which significantly reduces system performance and reliability [9]. So, Identifying the features that are most informative for intracranial hemorrhage classification is essential.

# Chapter 3

## Methodology

Diagnosing intracranial hemorrhage from CT DICOM images manually is challenging, and conducting hemorrhage assessments through traditional methods is costly. Neurologists and physicians emphasize that rapidly determining the subtype of hemorrhage can significantly impact their decision-making process when evaluating emergency patients or identifying crucial outcomes in the final stages of treatment. Various machine-learning techniques have been employed for the detection and diagnosis of hemorrhage. These approaches have often relied on handcrafted features, extracted from relatively small datasets, for localizing and classifying hemorrhage.

However, the application of such techniques to a broader and more diverse population can introduce significant errors, potentially leading to misdiagnoses and inadequate management. The current CNN models employed for ICH classification come with several shortcomings. They rely on subpar feature extraction techniques, which lead to the selection of inadequate features. Current convolutional neural network (CNN) models used for intracranial hemorrhage classification face shortcomings, particularly in their feature extraction techniques. The limitations in feature extraction can result in the selection of inadequate features, compromising the model's ability to accurately localize and classify hemorrhages. This issue is particularly critical in emergencies where the rapid and precise determination of intracranial hemorrhage subtypes is essential for effective decision-making in

patient care.[19, 23, 48–50]. Moreover, the process of feature extraction encounters the curse of dimensionality, resulting in substantial computational overhead [19, 23, 48–51]. Another limitation lies in the incorporation of poorly balanced and denormalized data, which hampers the model’s ability to generalize effectively in multiclass classification scenarios [23, 49].

Additionally, the use of small datasets is a primary factor contributing to model underfitting in supervised learning. To overcome the challenges associated with manual diagnosis and traditional methods, there has been a growing emphasis on leveraging machine-learning techniques for the detection and diagnosis of intracranial hemorrhage. Traditional approaches often relied on handcrafted features extracted from limited datasets, leading to suboptimal performance when applied to a broader and more diverse population.

Addressing these concerns, our approach goes beyond conventional CNN models. By employing advanced architectures such as the Attention U-Net, we enhance feature extraction, enabling the model to capture intricate patterns and details crucial for accurate hemorrhage localization and classification. This method aims to improve the overall diagnostic accuracy, especially in emergency scenarios, where timely and precise diagnosis significantly impacts patient outcomes.

Our approach centers on the utilization of the Attention U-Net model, a deep learning architecture that combines the strengths of CNNs and attention mechanisms to efficiently detect and classify brain hemorrhages and their subtypes. The Attention U-Net model we employ comprises two main components: an encoder and a decoder. The encoder is responsible for extracting pertinent features from the input image, while the decoder reconstructs the image using these extracted features. An attention mechanism is integrated to guide the decoder’s focus towards the most relevant regions within the image. In addition to the Attention U-Net model, our methodology involves various techniques and stages. Furthermore, addressing the challenge of limited data, we implement augmentation techniques to diversify and enrich our dataset, promoting better generalization during model training. Augmentation involves applying transformations to the existing images, such as rotations, flips, and scaling, thereby generating variations that

aid the model in learning robust features. To enhance feature selection and focus on critical regions, attention gates are incorporated into our Attention U-Net model. These attention gates dynamically modulate the importance of different features, allowing the model to selectively emphasize relevant details for accurate segmentation.

Our comprehensive methodology extends beyond architecture design. Leveraging the power of the Attention U-Net, we prioritize each step, ensuring the extraction of meaningful features, effective segmentation, and accurate classification. The integration of these components, along with meticulous preprocessing and augmentation, collectively fortifies our approach to intracranial hemorrhage detection and classification in CT scans.

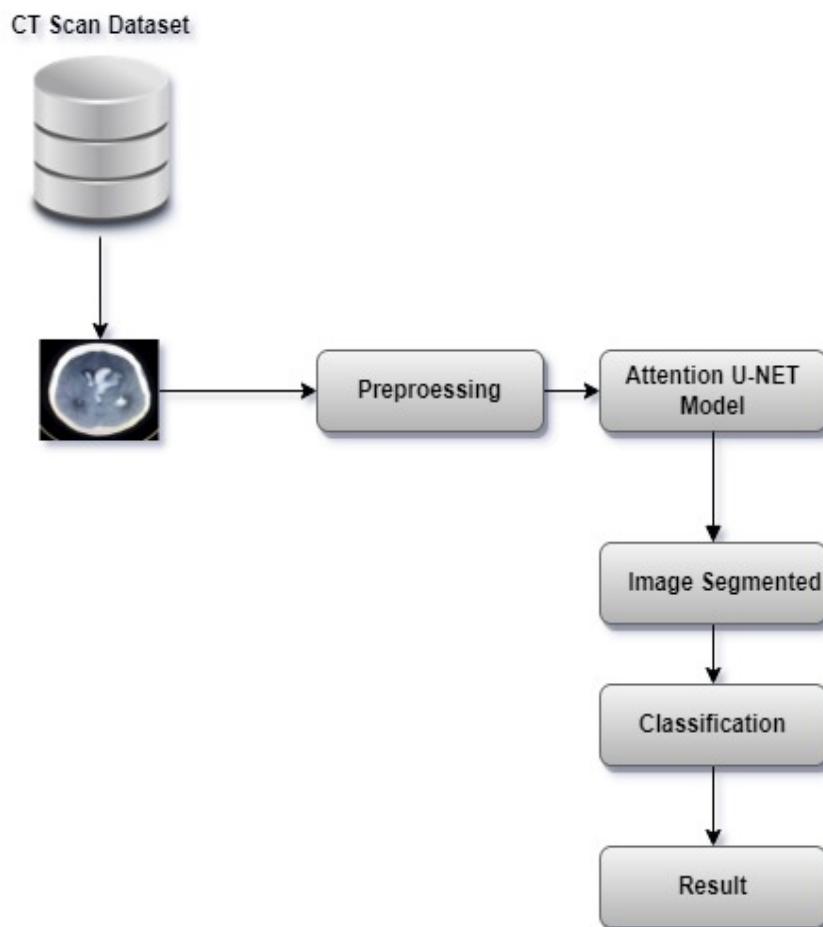


FIGURE 3.1: Proposed Methodology

In the initial phase of our methodology, we implemented a data augmentation technique to enrich the dataset's diversity, employing strategies to balance the dataset

effectively. Subsequently, we transformed DICOM images into Hounsfield Units (HU), a crucial step in preparing the data for further analysis. The conversion to HU enables standardized representation across different scanners and enhances comparability. Following the HU conversion, we applied windowing techniques to focus on specific ranges of HU values, optimizing the visualization and analysis of CT scans. This windowing step improves the clarity of relevant structures, emphasizing areas of interest while mitigating noise. Post-windowing, we carried out normalization on the images, scaling pixel values to a standardized range. Normalization is instrumental in ensuring consistent and comparable pixel intensity levels across images. After these preprocessing steps, we employed an Attention U-Net model, integrating attention mechanisms for feature selection and segmentation. In the final stage of our methodology, we executed the classification of intracranial hemorrhage subtypes. This comprehensive approach, from data augmentation to classification, ensures robust preprocessing and feature extraction, contributing to the model's efficacy in accurate hemorrhage localization and classification.

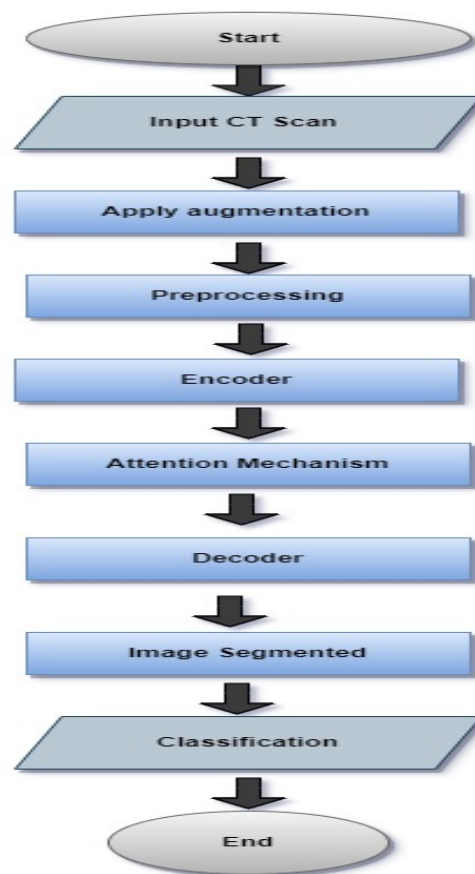


FIGURE 3.2: Flowchart of Proposed Methodology

### 3.1 Datasets

The RSNA dataset is the largest publicly available dataset of brain CT images annotated for hematoma detection and classification. The dataset consists of 874,035 images, which were annotated by expert radiologists for the presence or absence of five types of hematoma:

1. Intraparenchymal Hemorrhage (IPH)
2. Epidural Hemorrhage (EDH)
3. Subdural Hemorrhage (SDH)
4. Subarachnoid Hemorrhage (SAH)
5. Intraventricular Hemorrhage (IVH)

The training set consists of 752,803 images, and the test set consists of 121,232 images. The dataset has a class imbalance, meaning that some types of hematoma are more common than others[24].

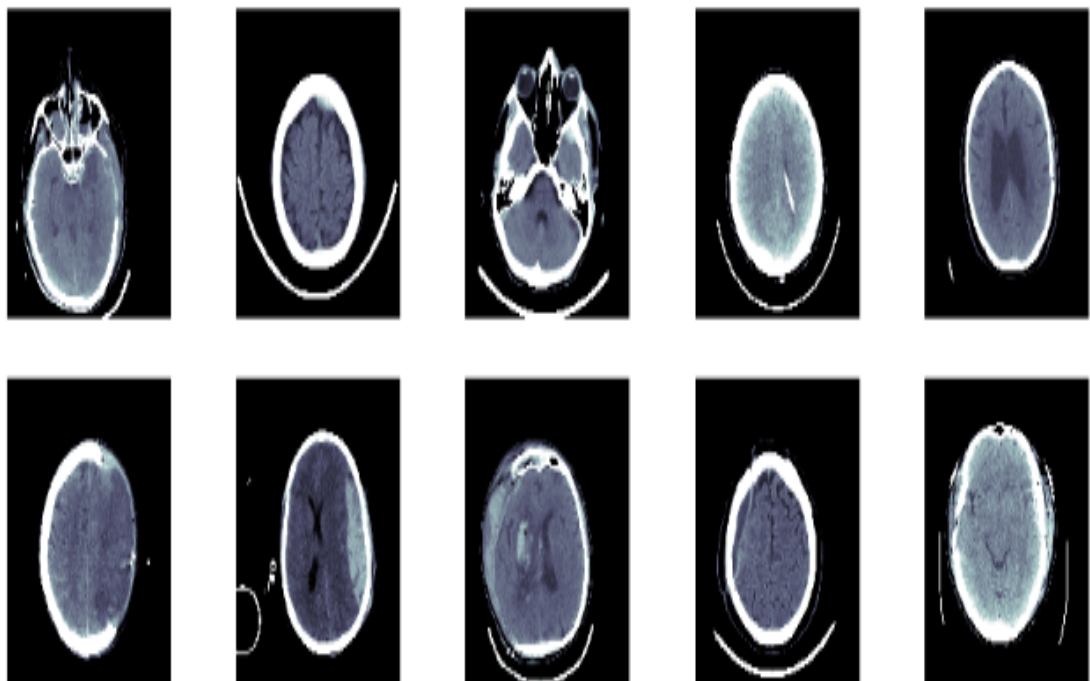


FIGURE 3.3: Epidural Hemorrhage(EDH)

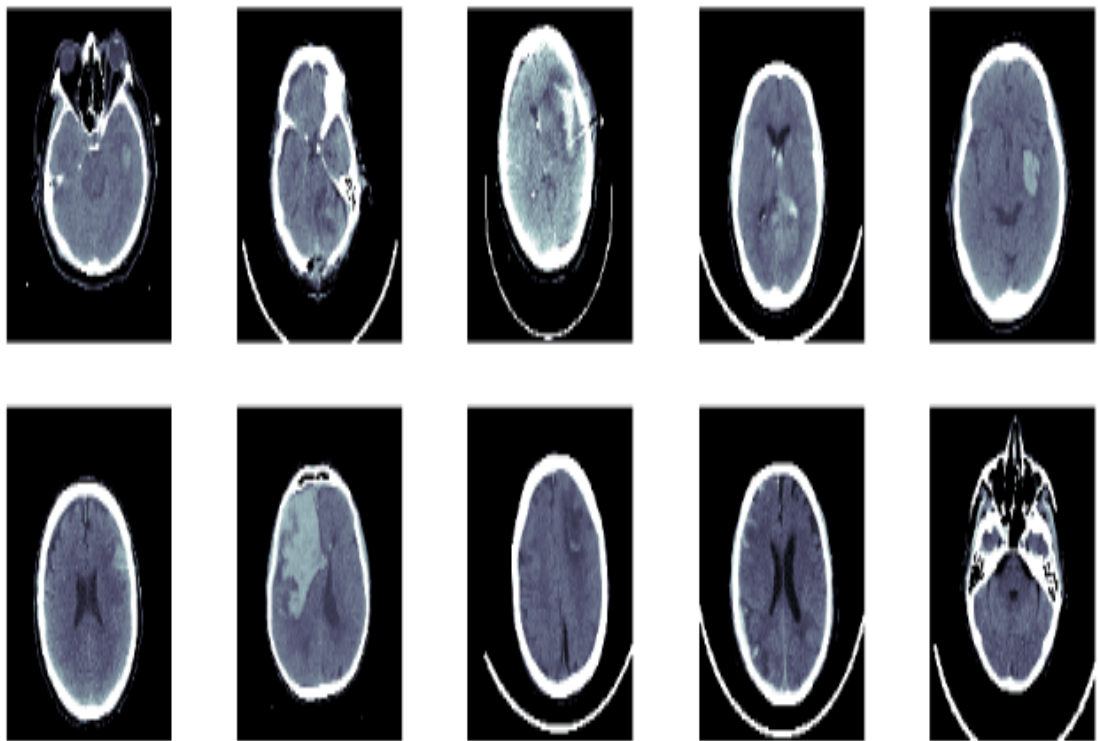


FIGURE 3.4: Intraparenchymal Hemorrhage (IPH)

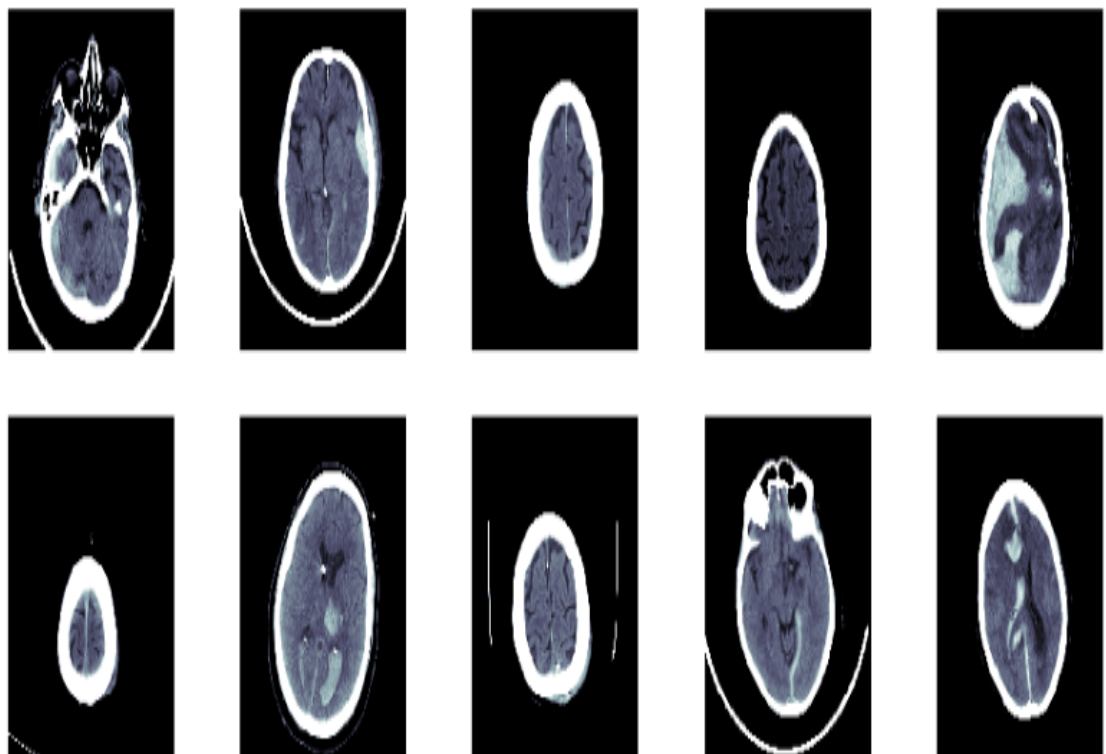


FIGURE 3.5: Subdural Hemorrhage (SDH)



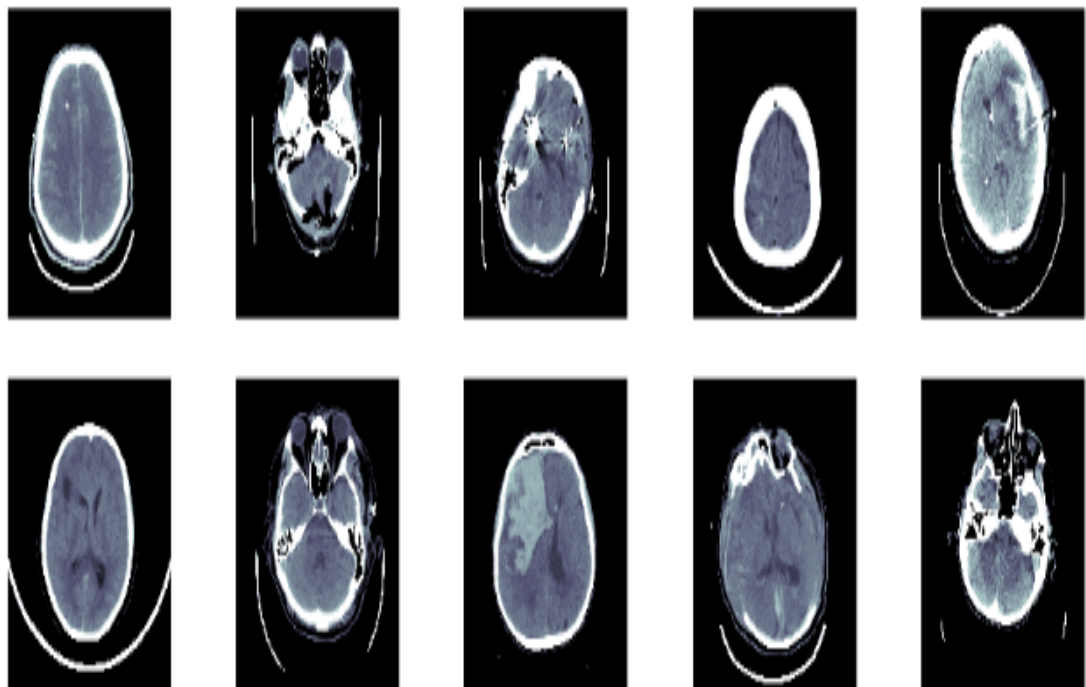


FIGURE 3.6: Subarachnoid Hemorrhage (SAH)

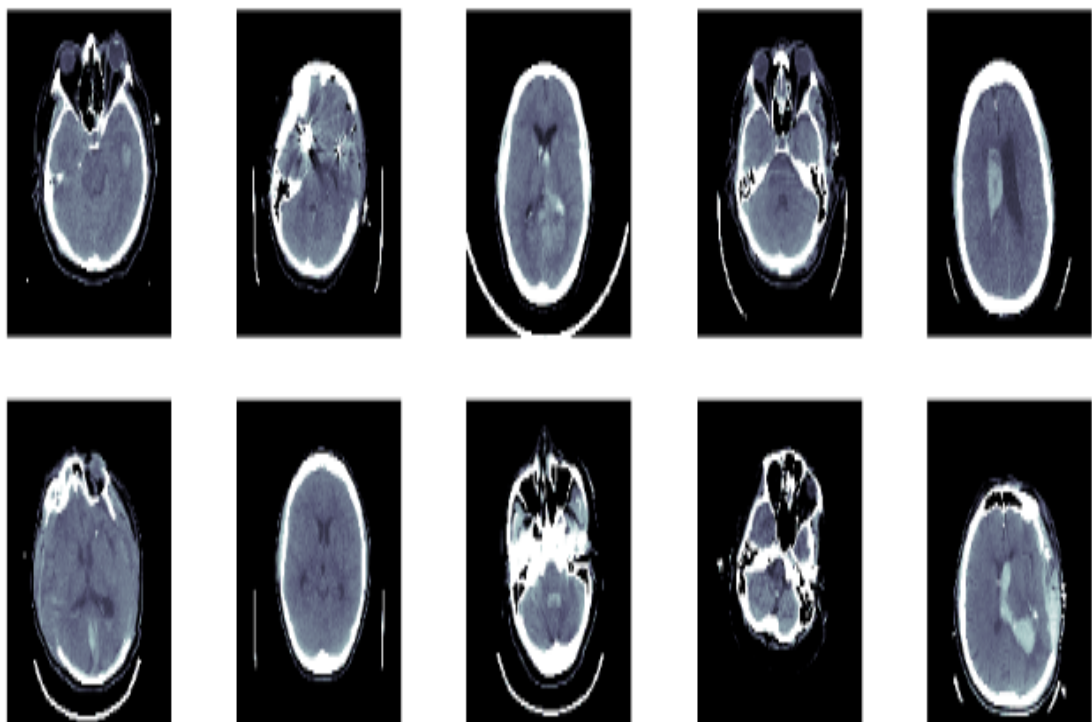


FIGURE 3.7: Intraventricular Hemorrhage (IVH)

### 3.1.1 Challenges

Challenges included in this dataset are as follows:

1. The primary challenge lies in training a model with significantly imbalanced class distributions. Among the five different types of intracranial hemorrhages, subdural hemorrhages are abundantly represented with 47,166 DICOM images, while epidural hemorrhages are notably underrepresented with just 3,145 DICOM images in the dataset.
2. The secondary challenge revolves around the existence of mutually exclusive labels, signifying instances where specific images showcase the simultaneous presence of multiple types of hemorrhages. This scenario introduces complexity in accurately categorizing and delineating the distinct hemorrhage subtypes within the dataset. Addressing this challenge necessitates sophisticated strategies to comprehensively capture and classify the diverse combinations of hemorrhage types evident in certain images, further enhancing the robustness of the analysis

To tackle these challenges, we formulated two distinct datasets: Dataset 1 and Dataset 2. This deliberate design facilitates a nuanced exploration of various scenarios, offering valuable insights into the intricate challenges linked to the presence of mutually exclusive labels within medical image datasets. By structuring the datasets with careful consideration for these labels, our approach not only enhances the understanding of such complexities but also sets the stage for more robust and insightful analyses in the realm of medical image classification.

Dataset 1 was carefully curated to eliminate mutually exclusive labels, ensuring that each DICOM file exclusively represents a single type of hemorrhage or none at all. Refer to Table 3.1 for a comprehensive breakdown of the image distribution across various hemorrhage types in Dataset 1.

In contrast, Dataset 2 was intentionally structured to incorporate mutually exclusive labels, enabling a single DICOM file to encompass multiple hemorrhage types

or none. The distribution of images for each type in Dataset 2 is outlined in Table 3.2.

TABLE 3.1: Intracranial Hemorrhage Dataset 1

Type Of Hemorrhage	DICOM image Number
Subdural	32200
Subarachnoid	16423
Intraventricular	9878
Intraparenchymal	15664
Epidural	1649
Normal Image	644870

TABLE 3.2: Intracranial Hemorrhage Dataset 2

Type Of Hemorrhage	DICOM image Number
Subdural	47166
Subarachnoid	35675
Intraventricular	26205
Intraparenchymal	36118
Epidural	3145
Normal Image	644870

Notably, Epidural hemorrhages exhibit underrepresentation, with only 3,145 DICOM images in the dataset. To address class imbalance concerns, we decided to exclude Epidural hemorrhages from our analysis. Additionally, we applied the Augmentation technique to balance the data, with a specific emphasis on augmenting the Intraventricular Hemorrhage class. This augmentation process resulted in the generation of additional images, contributing to a more balanced and representative dataset for our subsequent analyses.

In Dataset 1, we meticulously ensured a consistent count of 15,000 DICOM images for each class, as summarized in Table 3.3. For Dataset 2, our goal was to have 30,000 DICOM images for each type. However, due to random selection during the augmentation process, some duplicate files emerged. After eliminating these

duplicates, the revised counts are presented in Table 3.4 for clarity. This thorough approach to dataset creation and balancing establishes a robust groundwork for subsequent analyses and model training, effectively addressing challenges such as class imbalance and the complexities associated with mutually exclusive labels.

TABLE 3.3: Intracranial Hemorrhage Balance Dataset 1

Type Of Hemorrhage	DICOM image Number
Subdural	15000
Subarachnoid	15000
Intraventricular	15000
Intraparenchymal	15000
Normal Image	15000
Total Number of Images	75000

TABLE 3.4: Intracranial Hemorrhage Balance Dataset 2

Type Of Hemorrhage	DICOM image Number
Subdural	35007
Subarachnoid	33220
Intraventricular	30000
Intraparenchymal	33960
Normal Image	30000
Total Number of Images	120858

## 3.2 Data Pre-Processing

Data preprocessing is a fundamental step in preparing raw data for analysis or machine learning tasks. It involves a series of operations and transformations to clean, format, and organize the data so that it becomes suitable for further analysis or model training. Key steps in data preprocessing include cleaning, handling missing data, encoding categorical variables, scaling numerical features, and splitting the data into training and testing sets. These steps collectively contribute to

ensuring the quality and compatibility of the data for effective analysis and model performance.

### 1. **Correct DICOM Images:**

Correcting DICOM (Digital Imaging and Communications in Medicine) images is an important step in medical image processing to ensure that the images are properly formatted and have accurate pixel values. This correction process is particularly important in cases where DICOM images have certain issues, such as non-standard pixel values, incorrect scaling, or other anomalies. The first step is to read the DICOM image file. The DICOM image file is a standard format for storing and transmitting medical images. It contains a header that stores information about the image, such as the patient's name, the date the image was taken, and the type of scanner that was used. The DICOM image file also contains a pixel array that stores the values of the pixels in the image.

The next step is to check the `BitsStored` and `PixelRepresentation` tags in the DICOM header. The `BitsStored` tag specifies the number of bits used to store each pixel value in the image. The `PixelRepresentation` tag specifies whether the pixel values are stored in signed or unsigned format.

If the `BitsStored` tag is 12 and the `PixelRepresentation` tag is 0, then the `RescaleIntercept` tag is corrected. The `RescaleIntercept` tag is a value that is subtracted from each pixel value in the image. It is used to correct for the offset of the pixel values.

If the `RescaleIntercept` tag is not correct, then the image will be corrupted or have incorrect values. In this case, the `RescaleIntercept` tag can be corrected by adding 1000 to each pixel value in the image.

### 2. **Windowing:**

Windowing is a technique used to improve the contrast of an image by adjusting the range of pixel values that are displayed. It is done by multiplying the pixel values in the image by a slope and adding a bias. The slope and bias are chosen to highlight the desired features in the image. In medical images,

each pixel or voxel is assigned an intensity value based on the attenuation of X-rays (CT scans), signal intensity (MRI), or X-ray absorption (X-rays). These intensity values represent the density or composition of the tissues being imaged.

- (a) Window Width (WW): This parameter determines the range of intensity values that will be mapped to the full range of colors (usually grayscale) in the final displayed image. It controls the image's contrast.
- (b) Window Level (WL): Also known as the center, this parameter sets the midpoint of the intensity range that will be mapped to the middle shade of gray. It controls the image's brightness.

By adjusting the WW and WL settings, radiologists and medical professionals can focus on specific anatomical structures or pathological conditions. A narrow WW and WL may be used to visualize fine details in the brain, such as blood vessels or small lesions. A wide WW and a high WL may be used to clearly depict bones while suppressing soft tissues. Different WW and WL settings may be used to distinguish between various abdominal organs and pathologies.

use of three different intensity windows, each defined by its specific Window Level (L) and Window Width (W): the subdural window (L = 80 and W = 200) This window setting is likely used to visualize and highlight structures or pathologies related to subdural regions within the medical images. The L value of 80 sets the midpoint of the intensity range, while the W value of 200 determines the range of intensity values for contrast. This window configuration may be useful for detecting and assessing subdural hemorrhages, which have different radiodensity characteristics compared to other tissues.

., Soft window (L = 50 and W = 350)The soft window configuration is likely employed to visualize and emphasize soft tissues within the medical images. Soft tissues typically have moderate radiodensity, and this window setting optimizes the contrast to make them more prominent. It can be valuable for examining organs and structures like muscles and organs in the abdomen., and brain window (L = 40 and W = 80) The brain window setting is tailored to enhance the visualization of brain tissue. It provides

a narrow window width, making it suitable for highlighting fine details in brain imaging, including detecting abnormalities like lesions or infarctions. The L value of 40 sets the center of the intensity range.

### 3. Normalization:

Normalization is a critical preprocessing step in medical image analysis that aims to standardize the pixel intensity values within an image. It ensures that the pixel values have a consistent and comparable scale, which is essential for accurate and effective image analysis, feature extraction, and model training. Normalization is the process of scaling pixel values to a specific range, often between 0 and 1. This is typically done to ensure that the pixel values are in a consistent range, which can be helpful for neural networks during training. The normalize function is used to normalize the pixel values after windowing. It uses the minimum and maximum values from the windowed image to perform the normalization.

### 4. BSB (Brain, Subdural, Soft Tissues) Windowing:

BSB windowing is a specialized technique employed in medical imaging, particularly for CT scans, to fine-tune window level and width settings, thereby enhancing the visualization of distinct tissues and pathologies. This technique is particularly beneficial for visualizing brain tissue, subdural hematomas, and soft tissues. The process involves combining windowing and normalization for three specific tissue types: brain, subdural, and soft tissues. This integration results in a color image where each channel corresponds to one of these tissues. The strategic adjustment of window level and window width settings empowers radiologists and medical professionals to optimize the display, facilitating a clearer visualization of relevant structures or conditions. This tailored approach aids in the detection of abnormalities and contributes to a more comprehensive assessment of patient health.

### 5. Resizing the image:

Deep learning models often demand substantial computational resources. Larger input images contribute to increased parameters and computational

load, potentially taxing hardware resources and impeding the efficiency of both training and inference processes. To mitigate this challenge, resizing input images to a smaller dimension is employed to reduce computational complexity. In the context of this study, the original CT images, initially sized at  $512 \times 512 \times 3$ , have undergone a resizing transformation, resulting in dimensions of  $224 \times 224 \times 3$ . This resizing operation not only facilitates more manageable computational requirements but also streamlines the overall processing efficiency of the deep learning model.

### 3.3 Proposed Model

In this research study, we have introduced a novel Attention U-Net Model, which is specifically designed for the task of Multi-Class Image Classification. This innovative model builds upon the foundation of the Attention U-Net architecture, a powerful neural network structure for image segmentation. However, we have extended its capabilities by incorporating a classification layer, effectively modifying the model's original behavior and allowing it to excel in the context of image classification tasks.

The primary motivation for this research is to harness the strengths of the Attention U-Net architecture, which is renowned for its ability to capture fine-grained details in images, and adapt it for the challenges posed by multi-class image classification. By integrating a classification layer, our approach leverages the power of attention mechanisms while also enabling the model to make explicit class predictions, making it a valuable tool for a wide range of image classification tasks. This hybrid model represents a significant advancement in the field of computer vision, offering enhanced performance and accuracy for multi-class image classification scenarios.

The Attention U-Net is a convolutional neural network (CNN) architecture that seamlessly integrates the U-Net structure with attention mechanisms. The U-Net's distinctive dual-path design encompasses a contracting path and an expansive path. Within the contracting path, encoder layers capture contextual details



and reduce the spatial dimensions of the input. In contrast, the expansive path employs decoder layers responsible for decoding the encoded information. These decoder layers utilize skip connections to incorporate data from the contracting path, ultimately generating a segmentation map.

Attention, as a technique, enables the model to selectively focus on the most crucial parts of an image. This capability proves invaluable for various tasks such as image classification, object detection, and segmentation. By integrating attention mechanisms into the U-Net architecture, the Attention U-Net model enhances its capacity to prioritize significant features, contributing to improved performance in tasks requiring nuanced visual understanding. There are two main types of attention:

1. **Hard Attention:** Hard attention is a binary operation, meaning it makes a strict decision on whether to attend to a particular part of the image or not. This can be implemented by either cropping the image to exclusively include the identified crucial parts or by utilizing a mask to explicitly specify which regions of the image should be attended to. In hard attention, the focus is distinctly on selective, isolated areas without any gradation.
2. **Soft Attention:** Soft attention, in contrast, is a continuous operation that allows for a more nuanced approach to image attention. It enables the model to assign varying levels of attention to different parts of the image. This is achieved by assigning weights to different regions of the image, where higher weights indicate a greater degree of attention. Soft attention allows for a smoother, gradient-based distribution of attention across the image, providing flexibility in emphasizing different levels of importance to various regions.

### 3.3.1 Model Component

In the U-Net model, a key architectural element involves the utilization of skip connections to convey spatial information from the down-sampling network (encoder)

to the up-sampling network (decoder). While these connections play a crucial role in preserving detailed information and context, they can introduce suboptimal feature representations, particularly when dealing with information from the early layers of the network. To overcome this challenge, the introduction of attention gates by [25] marks a significant enhancement to the model.

The integration of attention gates represents a noteworthy advancement in the U-Net architecture. These attention gates serve a critical purpose by selectively suppressing activations that are deemed less relevant. This innovative addition substantially improves feature representation, especially when dealing with information from the initial layers. Consequently, attention gates not only address the challenge of suboptimal feature representations but also significantly enhance overall segmentation performance.

The integration of attention gates in the U-Net model introduces a sophisticated mechanism that plays a pivotal role in refining the model's decision-making process. Attention gates operate by selectively emphasizing or de-emphasizing features, enabling the U-Net to discern and prioritize relevant information. This nuanced feature selection enhances the model's ability to capture critical details, particularly in the presence of complex and intricate image structures. Moreover, attention gates contribute to addressing the inherent challenges associated with information from the early layers of the network. By selectively suppressing less relevant activations, attention gates mitigate the risk of suboptimal feature representations. This selective attention mechanism ensures that the U-Net not only maintains its prowess in preserving fine-grained details through skip connections but also elevates its overall segmentation performance.

The impact of attention gates extends beyond the U-Net architecture's conventional capabilities, offering a versatile solution for improved semantic segmentation and image analysis. The model's adaptability to different domains and scenarios is heightened, making it a valuable tool for applications where discerning and prioritizing features is crucial. This innovative addition propels the U-Net model into the forefront of advanced image processing, reinforcing its reputation as a cutting-edge solution for complex segmentation tasks.

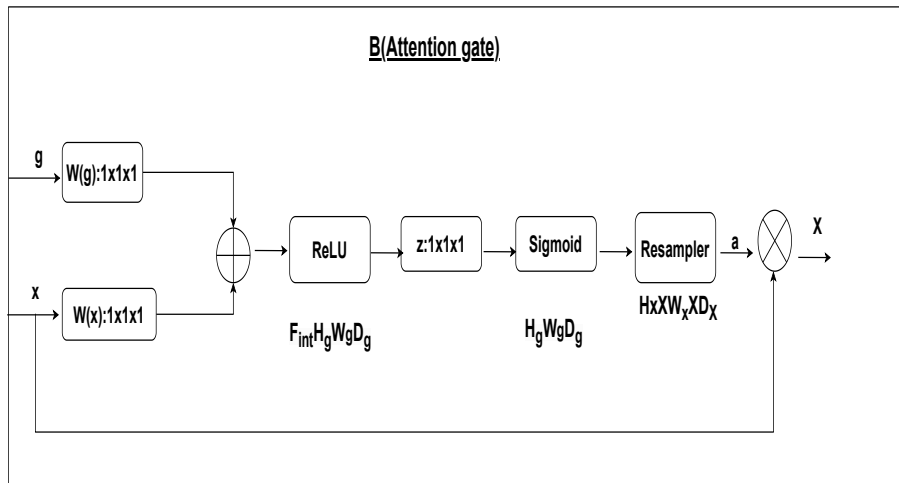
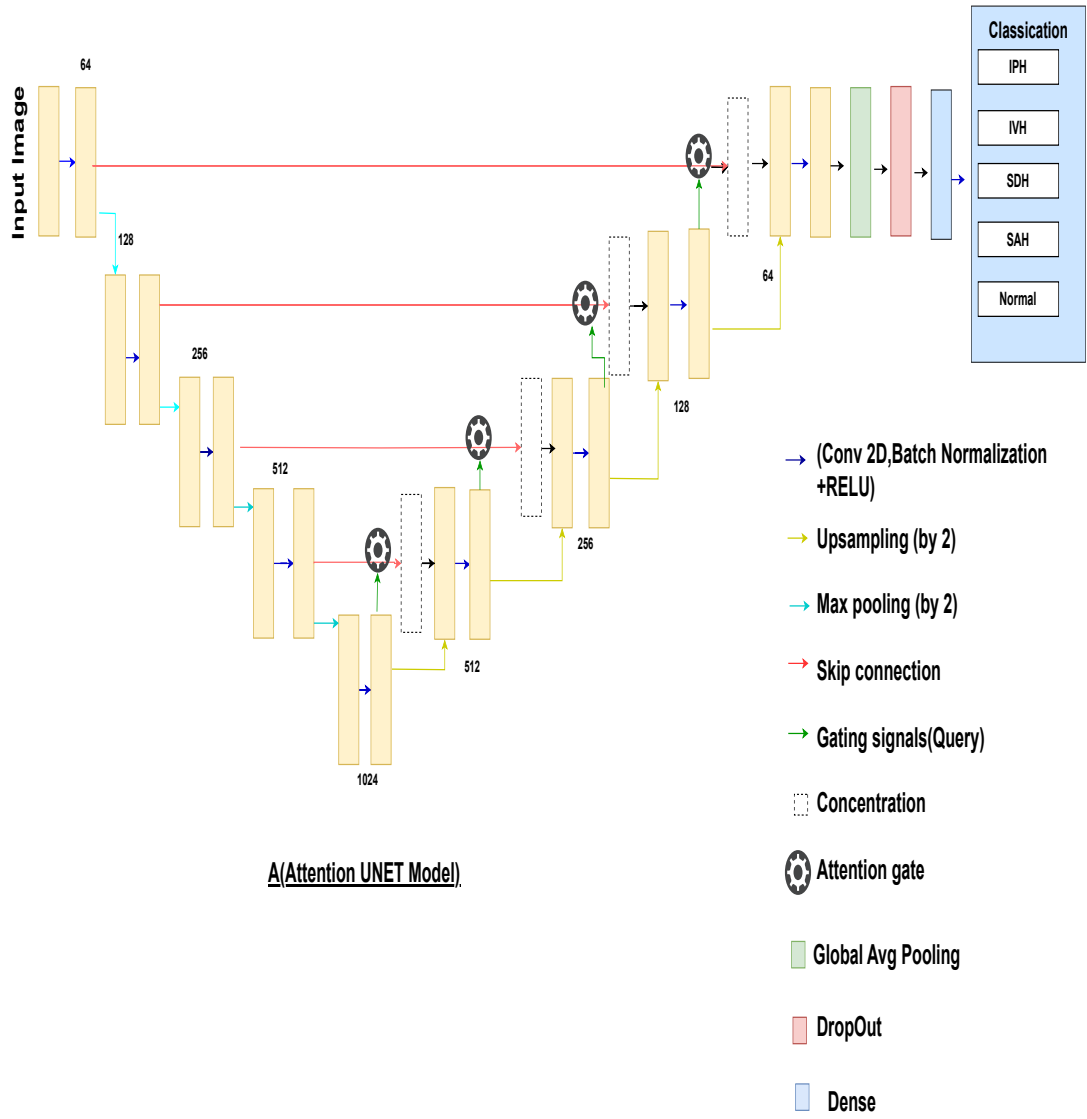


FIGURE 3.8: Attention U-NET for Classification

### 1. **Contraction Path:**

The contraction path within the architecture of the Attention U-Net model serves a pivotal role in the feature extraction process from the input image. It comprises a sequence of convolutional layers, coupled with subsequent max pooling layers, and its function is integral to the model's ability to capture relevant image features effectively.

The convolutional layers situated along the contraction path operate hierarchically. They are responsible for the extraction of features from the input image, and this process unfolds in a multi-scale manner. The lower-level convolutional layers focus on capturing elementary features such as edges, corners, and fine-grained textures. These fundamental features provide the building blocks for more intricate representations. As we ascend through the network's architecture, the convolutional layers become increasingly adept at capturing high-level features, including complex objects, shapes, and semantic information. This hierarchical feature extraction enables the model to progressively learn and represent both fine-grained and contextually rich aspects of the input data. Max pooling layers, integrated within the contraction path, play a crucial role in downsampling the feature maps produced by the convolutional layers. This downsampling reduces the spatial dimensions of the feature maps, resulting in a more compact representation. Beyond the computational efficiency benefits, downsampling can also facilitate the model in focusing on the most salient information while discarding redundant details. This contributes to the model's ability to capture and process features efficiently, making it well-suited for a wide range of computer vision and image analysis tasks.

In essence, the contraction path of the Attention U-Net model serves as the bedrock for its feature extraction capabilities. This path, comprising convolutional and max pooling layers, forms a crucial component that empowers the model to delve into the intricate details of the input image. Through this process, the model creates hierarchical representations that encapsulate essential features, setting the stage for subsequent tasks like image segmentation and classification. The combination of convolutional operations and

max pooling strategically applied in the contraction path allows the Attention U-Net to capture and distill key information, fostering a nuanced understanding of the input data that is pivotal for achieving accurate and effective results in downstream processes.

## 2. Attention Gate (AG):

An attention gate (AG) is a neural network that is used to weight the features extracted by the encoder in the Attention U-Net model. The AG takes as input the features extracted by the encoder and outputs a gating signal that is used to weight the features.

The attention gates within the model take input from two sources: one originates from the immediately preceding lower-level network layer (denoted as 'g'), and the other originates from skip connections (referred to as 'x'). The 'x' input, coming from a layer one level above, has double the height (H) and width (W) dimensions. To align these dimensions before combining them, we apply a convolution operation to 'x' with a stride of 2. Afterward, we perform element-wise addition, followed by rectified linear unit (ReLU) activation. Subsequently, we use a convolution operation with a single (1,1) filter and apply a sigmoid activation function. This step essentially computes the weights of attention. We then up-sample the resulting attention weights to match the dimensions of 'x'. Finally, we perform element-wise multiplication between the up-sampled attention weights and 'x'.

## 3. Expansion Path:

The expansion path in the Attention U-Net model is the part of the model that reconstructs the image from the features extracted by the encoder. The expansion path consists of a series of convolutional layers, followed by up-sampling layers. The convolutional layers in the expansion path reconstruct the image from the features extracted by the encoder. The features are reconstructed in a hierarchical manner, with the lower layers reconstructing low-level features, such as edges and corners, and the higher layers reconstructing high-level features, such as objects and shapes. The upsampling

layers in the expansion path upsample the features extracted by the convolutional layers. In the attention features from lower levels are brought up, and at the same level, feature maps are concatenated using skip connections. Description of the working of the expansion path in the Attention U-Net model are as follow.

- (a) Attention features, which capture important information from lower levels of the network, are up-sampled to match the spatial resolution of the current level.
- (b) Simultaneously, feature maps from the same level in the contracting (down-sampling) path, which contain both detailed spatial information and higher-level abstractions, are retained.
- (c) These two sets of features, the up-sampled attention features and the feature maps from the current level, are then concatenated.
- (d) The concatenation operation combines the valuable spatial details from the skip connections with the refined features obtained from the attention mechanism.
- (e) The resulting feature maps contain a fusion of contextual information and fine-grained spatial details, enhancing the network's ability to generate accurate segmentations.

This intricate process of attention-guided feature fusion within the Attention U-Net model is crucial for achieving high-quality image segmentations. By strategically combining the up-sampled attention features and the preserved feature maps from the down-sampling path, the model ensures that the segmented output encapsulates both the contextual richness derived from higher-level abstractions and the fine-grained spatial details originating from the skip connections.

The up-sampling of attention features allows the model to emphasize important information from the lower layers, capturing intricate details that might be crucial for accurate segmentation. Simultaneously, the retention of feature maps from the same level in the down-sampling path ensures that the

network retains comprehensive spatial information, balancing both detailed and abstract representations.

The subsequent concatenation operation serves as a fusion point, bringing together these two sets of features. This fusion not only preserves the spatial intricacies through skip connections but also incorporates refined attention-guided information. The resulting feature maps are a harmonious blend of contextual understanding and spatial precision, providing the Attention U-Net model with the capability to generate segmentations that accurately represent the complexities present in the input images.

---

**Algorithm 1:** Attention U-NET Algorithm
 

---

**Input:** Input Image  $I$

**Output:** Segmentation Mask  $M$

**function** Initialize():

**Initialize:** Contracting Path Layers (Encoder);

**Initialize:** Expansive Path Layers (Decoder);

**Initialize:** Attention Mechanism Layers;

Initialize();

**for**  $t = 1$  to  $T$  **do**

    Encode Image  $I$  with Contracting Path Layers;

    Apply Attention Mechanism to Encoded Features;

    Decode Encoded Features with Expansive Path Layers;

**return**  $M$ ;

---

### 3.4 Classification

Within our dataset, the absence of explicit segmentation masks posed a significant challenge. To address this, we adopted a novel approach by implementing an Attention-based U-Net model. This advanced model harnesses the power of attention gates to discern and capture vital features from the images, all without the dependency on manual segmentation masks. The outcome of this process results in the production of segmented images. To further our analysis, we incorporated

a classification layer into the workflow. This added layer of the model is instrumental in categorizing the segmented images into distinct subtypes of intracranial hemorrhage. By doing so, we are not only able to detect the presence of intracranial hemorrhage but also to differentiate between various subtypes, which can be crucial for medical diagnosis and treatment decisions.

What makes this approach particularly noteworthy is its ability to perform this classification task without the need for manual segmentation annotations. This means that even when explicit segmentation masks are unavailable, we can still effectively identify and classify intracranial hemorrhage subtypes in medical images, making the entire process more versatile and accessible for a broader range of medical imaging datasets and scenarios. Furthermore, the Attention-based U-Net model introduces a layer of interpretability into the classification process. The attention gates play a crucial role in highlighting specific regions of interest within the images, providing insights into the features that contribute most significantly to the model's classification decisions. This interpretability aspect is crucial in medical contexts, where understanding the basis of classification can enhance the trust and adoption of the model by healthcare professionals.

Moreover, the Attention-based U-Net model exhibits a robust generalization capability, demonstrating consistent performance across diverse datasets. Its ability to adapt to different datasets without the need for extensive manual annotation or segmentation makes it a valuable tool for various medical imaging scenarios.

### 1. **Global Average Pooling 2D:**

This layer performs global average pooling on the feature maps from the previous layers. It helps in reducing the spatial dimensions of the feature maps to a single value per feature, which is important for classification.

### 2. **Dropout:**

Dropout is a regularization technique used to prevent overfitting in neural networks. It randomly sets a fraction of input units to zero during each update, which helps reduce the risk of the model relying too heavily on specific features.



### 3. Dense:

The final layer is a fully connected dense layer. It takes the output from the previous layers and performs the actual classification. The dense layer uses a softmax activation function, which outputs a probability distribution over the classes.

---

#### **Algorithm 2:** Image Classification Algorithm

---

**Input:** Segmentation Mask  $M$ , Number of Classes ( $num\_classes$ )

**Output:** Subtype label prediction

**function** Initialize():

    | **Initialize:** Number of Classes  $\leftarrow 5$ ;

Initialize();

**for**  $t = 1$  to  $T$  **do**

    | Apply GlobalAveragePooling2D Layer (GAP) to Segmentation Mask  $M$  ;

    | Apply Dropout Layer (Dropout) with a dropout rate of 0.8;

    | Apply Dense Layer (Dense) with  $num\_classes$  units and softmax  
    | activation;

    | Return the Predicted Class Probability Vector ( $P$ );

**return**  $P$ ;

---

## 3.5 Benchmark Techniques

### 3.5.1 Mobile-Net

MobileNet is a convolutional neural network (CNN) architecture developed by Howard et al. in 2017. It is a type of lightweight CNN that is designed for mobile devices. MobileNet uses a technique called depthwise separable convolutions to reduce the number of parameters and computations required.

MobileNet has 28 layers, which are arranged in 13 blocks. Each block consists of a depthwise separable convolution, followed by a pointwise convolution. The depthwise separable convolution is a type of convolution that splits the input into

channels and then performs a convolution on each channel independently. Pointwise convolution is a type of convolution that combines the output of the depthwise separable convolution into a single channel. The first layer of MobileNet is a convolutional layer with 32 filters and a 3x3 kernel. The output of this layer is then passed through a max pooling layer with a 2x2 kernel and a stride of 2. The next 12 blocks are arranged in a sequential manner. Each block consists of a depthwise separable convolution, followed by a pointwise convolution. The depthwise separable convolution uses 16, 32, 64, 128, or 256 filters, depending on the block. The pointwise convolution uses the same number of filters as the depthwise separable convolution. The last layer of MobileNet is a global average pooling layer, followed by a fully connected layer with 1000 outputs. The 1000 outputs correspond to the 1000 classes in the ImageNet dataset. This model is particularly efficient in image classification tasks because of its utilization of inverted residual blocks, which manage to achieve outstanding results while maintaining a more modest parameter count.

To harness the power of MobileNet for the specific task of classifying intracranial hemorrhage (ICH) subtypes, we employed a transfer learning approach. By fine-tuning the model on our dataset, we were able to leverage its robust pre-trained features for our classification task, ultimately benefiting from its capacity to recognize intricate patterns in medical images.

Layer (type)	Output Shape	Param #
input_layer (InputLayer)	[(None, 224, 224, 3)]	0
mobilenet_1.00_224 (Functional)	(None, None, None, 1024)	3228864
global_average_pooling2d_1 (GlobalAveragePooling2D)	(None, 1024)	0
dropout_1 (Dropout)	(None, 1024)	0
dense_1 (Dense)	(None, 5)	5125
=====		
Total params: 3,233,989		
Trainable params: 3,212,101		
Non-trainable params: 21,888		
=====		
None		

FIGURE 3.9: MobileNet Model Diagram

### 3.5.2 Dense-Net 121

DenseNet, short for Dense Convolutional Network, is a sophisticated neural network architecture meticulously crafted to enhance the depth of deep learning models while simplifying the training process. This innovation is achieved through the integration of shorter connections between layers, creating a unique densely connected structure within the model. Unlike traditional convolutional neural networks (CNNs), each layer in DenseNet is directly linked to all subsequent layers, forming an intricate web of connections.

A notable advantage of DenseNet lies in its ability to significantly reduce the number of parameters required compared to conventional CNNs. This efficiency stems from the avoidance of redundant feature mappings across layers, resulting in a streamlined and resource-efficient architecture. Consequently, DenseNet has emerged as a highly effective and widely embraced neural network design across various applications.

Within the DenseNet architecture, the concept of a dense block takes center stage, comprising layers that are repeated within the block to achieve varying depths. Each of these layers follows a specific design, incorporating two convolutions. The first convolution employs a 1x1-sized kernel, serving as a bottleneck layer, followed by a 3x3 kernel for the core convolution operation. This strategic design enhances feature extraction and promotes efficient information flow within the network, contributing to the overall success and popularity of DenseNet in the field of deep learning.

Moreover, every transition layer within the DenseNet model contains a 1x1 convolutional layer and a 2x2 average pooling layer with a stride of 2. This results in DenseNet-121 having the following layers in its architecture: one 7x7 Convolution layer, fifty-eight 3x3 Convolution layers, sixty-one 1x1 Convolution layers, four Average Pooling layers, and one Fully Connected Layer. Altogether, this architecture comprises 120 convolutional layers and 4 average pooling layers, culminating in a comprehensive network structure. To harness the power of DenseNet for the specific task of classifying intracranial hemorrhage (ICH) subtypes, we employed a

transfer learning approach. By fine-tuning the model on our dataset, we were able to leverage its robust pre-trained features for our classification task, ultimately benefiting from its capacity to recognize intricate patterns in medical images.

Layer (type)	Output Shape	Param #
input_layer (InputLayer)	[(None, 224, 224, 3)]	0
densenet121 (Functional)	(None, None, None, 1024)	7037504
global_average_pooling2d (GlobalAveragePooling2D)	(None, 1024)	0
dropout (Dropout)	(None, 1024)	0
dense (Dense)	(None, 5)	5125
=====		
Total params: 7,042,629		
Trainable params: 6,958,981		
Non-trainable params: 83,648		
=====		
None		

FIGURE 3.10: DenseNet121 Model Diagram

### 3.5.3 Dense-Net 169

DenseNet-169 is a variant of the Dense Convolutional Network architecture that builds upon the principles of DenseNet-121 but incorporates a more extensive set of layers. In DenseNet models, each dense block consists of multiple connected layers, where each layer receives inputs from all previous layers within the same block, creating dense connectivity. DenseNet-169 adheres to this design philosophy, featuring a substantial number of 3x3 convolutional layers within its dense blocks. These convolutional layers are equipped with bottleneck layers, typically including 1x1 convolutional layers, to reduce channel dimensions and computational complexity before forwarding data to subsequent layers. Transition layers are composed of 1x1 convolutional layers followed by average pooling layers, aiming to downsample the feature maps' spatial dimensions. DenseNet-169 has 169 layers, which are arranged in 16 dense blocks. Each dense block consists of 16 convolutional layers that are densely connected. The convolutional layers in each dense block use a 3x3 kernel and a stride of 1. The output of each dense block is

then concatenated with the output of the previous dense block. The first layer of DenseNet-169 is a convolutional layer with 64 filters and a 7x7 kernel. The output of this layer is then passed through a max pooling layer with a 3x3 kernel and a stride of 2. The next 16 dense blocks are arranged in a sequential manner. Each dense block consists of 16 convolutional layers that are densely connected. The convolutional layers in each dense block use a 3x3 kernel and a stride of 1. The output of each dense block is then concatenated with the output of the previous dense block. The last layer of DenseNet-169 is a global average pooling layer, followed by a fully connected layer that gives classification output. We employed a transfer learning approach. By fine-tuning the model on our dataset, we were able to leverage its robust pre-trained features for our classification task, ultimately benefiting from its capacity to recognize intricate patterns in medical images.

Layer (type)	Output Shape	Param #
input_layer (InputLayer)	[(None, 224, 224, 3)]	0
densenet169 (Functional)	(None, None, None, 1664)	12642880
global_average_pooling2d (GlobalAveragePooling2D)	(None, 1664)	0
dropout (Dropout)	(None, 1664)	0
dense (Dense)	(None, 5)	8325
=====		
Total params: 12,651,205		
Trainable params: 12,492,805		
Non-trainable params: 158,400		
=====		
None		

FIGURE 3.11: DenseNet-169 Model Diagram

### 3.5.4 ResNet 101

ResNet-101 is a convolutional neural network (CNN) architecture developed by He et al. in 2015. It is a type of deep residual network (ResNet) that uses residual connections. Residual connections help to address the problem of vanishing gradients, which can occur in deep neural networks. ResNet-101 has 101 layers,

which are arranged in 34 residual blocks. Each residual block consists of two convolutional layers that are connected by a residual connection.

The convolutional layers in each residual block use a 3x3 kernel and a stride of 1. The output of each residual block is then added to the input of the residual block. The first layer of ResNet-101 is a convolutional layer with 64 filters and a 7x7 kernel. The output of this layer is then passed through a max pooling layer with a 3x3 kernel and a stride of 2. The next 34 residual blocks are arranged in a sequential manner. Each residual block consists of two convolutional layers that are connected by a residual connection. The convolutional layers in each residual block use a 3x3 kernel and a stride of 1. The output of each residual block is then added to the input of the residual block. The last layer of ResNet-101 is a global average pooling layer, followed by a fully connected layer with 1000 outputs. The 1000 outputs correspond to the 1000 classes in the ImageNet dataset.

We employed a transfer learning approach. By fine-tuning the model on our dataset, we were able to leverage its robust pre-trained features for our classification task, ultimately benefiting from its capacity to recognize intricate patterns in medical images.

Layer (type)	Output Shape	Param #
input_layer (InputLayer)	[(None, 224, 224, 3)]	0
resnet101 (Functional)	(None, None, None, 2048)	42658176
global_average_pooling2d_1 (GlobalAveragePooling2D)	(None, 2048)	0
dropout_1 (Dropout)	(None, 2048)	0
dense_1 (Dense)	(None, 5)	10245
=====		
Total params: 42,668,421		
Trainable params: 42,563,077		
Non-trainable params: 105,344		
=====		
None		

FIGURE 3.12: ResNet-101 Model Diagram

### 3.5.5 ResNet 152

ResNet-152, a convolutional neural network (CNN) architecture introduced by He et al. in 2015, represents a pivotal advancement in deep learning. As a profound instantiation of a deep residual network (ResNet), it strategically incorporates residual connections to mitigate the challenge of vanishing gradients often encountered in deep neural networks.

Comprising an impressive 152 layers organized into 50 residual blocks, ResNet-152 employs a unique structure. Each residual block integrates two convolutional layers seamlessly connected by a residual connection. The convolutional layers within each block utilize a 3x3 kernel with a stride of 1, enhancing the network's capacity for feature extraction. Crucially, the output of each residual block is additive with the input, facilitating the unhindered flow of information through the network.

The initial layer of ResNet-152 initiates with a convolutional layer boasting 64 filters and a substantial 7x7 kernel. Following this, the output undergoes further processing via a max pooling layer with a 3x3 kernel and a stride of 2, optimizing feature extraction.

The subsequent 50 residual blocks are systematically arranged in sequence, preserving the two-convolutional-layer configuration connected by residual connections. These convolutional layers, again utilizing a 3x3 kernel and a stride of 1, continue to enhance the network's ability for intricate feature discernment. The additive integration of output and input remains a consistent design principle across all residual blocks.

The concluding layer of ResNet-152 features a global average pooling layer succeeded by a fully connected layer with 1000 outputs. These outputs align with the 1000 classes in the ImageNet dataset, showcasing the network's proficiency in image classification. The adoption of a transfer learning approach further leverages the pre-trained capabilities of ResNet-152, highlighting its adaptability and efficacy across diverse applications. By fine-tuning the model on our dataset, we were able to leverage its robust pre-trained features for our classification task,

ultimately benefiting from its capacity to recognize intricate patterns in medical images.

Layer (type)	Output Shape	Param #
input_layer (InputLayer)	[(None, 224, 224, 3)]	0
resnet152 (Functional)	(None, None, None, 2048)	58370944
global_average_pooling2d (GlobalAveragePooling2D)	(None, 2048)	0
dropout (Dropout)	(None, 2048)	0
dense (Dense)	(None, 5)	10245
=====		
Total params: 58,381,189		
Trainable params: 58,229,765		
Non-trainable params: 151,424		
=====		
None		

FIGURE 3.13: ResNet-152 Model Diagram

## 3.6 Evaluation

The assessment of various methods for classifying ICH subtypes follows a standard train-validation-test procedure. The training phase involves training the method on the designated training dataset, while the validation dataset is utilized to optimize hyperparameters and fine-tune the model. Subsequently, the performance of each system is rigorously evaluated on the independent test dataset to gauge its overall effectiveness.

### 1. Average F-score

The average F-score often denoted as F1-score or simply F-score, is a statistical measure used to assess the accuracy and precision of a classification model. It is calculated as the harmonic mean of precision and recall and provides a balance between these two metrics. It is a valuable metric for evaluating the overall performance of a classification model, especially in situations where a single accuracy score may not provide a complete picture



of its effectiveness. The F1-score serves as a valuable tool in the comprehensive evaluation of classification models, offering insights into their ability to achieve a harmonious blend of precision and recall. By considering both false positives and false negatives, the F1-score provides a more nuanced perspective on the model's overall performance. This makes it especially relevant in domains where the consequences of misclassifications are asymmetric, emphasizing the importance of a holistic evaluation approach.

In essence, the F1-score proves to be an indispensable metric for practitioners and researchers alike, contributing to a thorough and balanced assessment of classification models and their real-world applicability.

$$F_{\text{avg}} = \frac{2}{C} \sum_{c=1}^C \frac{\text{Recall}_c \cdot \text{Precision}_c}{\text{Recall}_c + \text{Precision}_c} \quad (3.1)$$

where  $C$  is the Number of classes and

$$\text{Recall}_c = \frac{TP_c}{TP_c + TN_c} \quad (3.2)$$

$$\text{Precision}_c = \frac{TP_c}{TP_c + FP_c} \quad (3.3)$$

## 2. Average Accuracy:

Average accuracy, in the context of machine learning and classification tasks, is a metric used to evaluate the overall performance of a model across multiple classes or categories. It is particularly relevant in multi-class classification scenarios.

The computation of average accuracy involves a two-step process. Firstly, accuracy is calculated for each specific class or category within the classification. This individual class accuracy is determined by the ratio of correctly predicted instances for that class to the total instances belonging to that class. Subsequently, the average accuracy is derived by taking the mean of these individual accuracies, providing a comprehensive assessment of the model's performance across all classes. In essence, average accuracy offers a

consolidated view of how well a model performs in distinguishing between different classes, making it a valuable metric for evaluating the overall effectiveness of a classification model in multi-class scenarios.

$$\text{Accuracy}_{\text{avg}} = \frac{1}{C} \sum_{c=1}^C \frac{TP_c + TN_c}{TP_c + FP_c + TN_c + FN_c} \quad (3.4)$$

### 3. True Positive Rate (TPR):

True Positive Rate (TPR), also known as Sensitivity, Recall, or Hit Rate, is a performance metric used in binary classification and medical diagnostics. It measures the proportion of actual positive cases that the model correctly identifies as positive.

$$TPR_{\text{avg}} = \frac{1}{C} \sum_{c=1}^C \frac{TP_c}{TP_c + FN_c} \quad (3.5)$$

### 4. True Negative Rate (TNR):

True Negative Rate (TNR), also known as Specificity, is a performance metric used in binary classification and medical diagnostics. It measures the proportion of actual negative cases that the model correctly identifies as negative.

$$TNR_{\text{avg}} = \frac{1}{C} \sum_{c=1}^C \frac{TN_c}{FP_c + TN_c} \quad (3.6)$$

# Chapter 4

## Implementation and Experiments of the Proposed Methodology

A detailed explanation of the proposed methodology can be found in Chapter 3. This chapter is dedicated to discussing the experiments conducted and the results obtained through the application of the proposed methodology.

### 4.1 Tools and Technology

#### 1. **Kaggle Jupyter Notebook:**

Kaggle Jupyter Notebook is a web-based environment that allows you to write and execute code in Python. It is a popular tool for machine learning experiments because it is easy to use and it provides a variety of features that are useful for data science, such as a code editor, a terminal, and a debugger.

#### 2. **Python programming language:**

Python stands as a versatile, general-purpose programming language renowned for its popularity in the field of machine learning. Widely embraced for its readability and simplicity, Python proves to be an accessible language for both beginners and experienced developers. One of its key strengths lies

in its extensive library ecosystem, which includes powerful tools and frameworks essential for machine learning endeavors.

Notably, Python serves as the foundation for prominent machine learning libraries like TensorFlow and Keras. TensorFlow, a widely-used open-source framework, is renowned for its flexibility and scalability in building and training deep learning models. Keras, on the other hand, operates as a high-level neural networks API, simplifying the process of model construction and training.

### 3. TensorFlow and Keras libraries:

TensorFlow and Keras stand out as prominent libraries in the realm of deep learning. TensorFlow serves as a foundational, low-level library that lays the groundwork for constructing intricate deep-learning models. Known for its versatility and robustness, TensorFlow offers a comprehensive set of tools for implementing various machine learning and deep learning algorithms. On the other hand, Keras is a high-level library that operates as an abstraction layer atop TensorFlow, simplifying the process of designing and training deep learning models.

Keras is particularly valued for its user-friendly interface, making it accessible to individuals with diverse levels of expertise in deep learning. Its high-level nature allows for a more intuitive and streamlined development experience, enabling practitioners to focus on model architecture and experimentation without delving into the intricacies of low-level implementation details.

### 4. Kaggle GPU:

Kaggle GPU stands as a valuable service offering access to Graphics Processing Units (GPUs) tailored for conducting machine learning experiments. Recognized for their superior speed in comparison to Central Processing Units (CPUs).

GPUs prove particularly advantageous in accelerating the training of deep learning models. This service becomes a cornerstone for data scientists and

researchers seeking efficient and high-performance computing resources to advance their experiments and analyses within the Kaggle platform.

## 4.2 Dataset

The RSNA (Radiological Society of North America) dataset stands as a significant and openly available repository of brain CT images with detailed annotations for hematoma detection and classification. This expansive dataset encompasses an impressive 874,035 images, each meticulously reviewed and annotated by expert radiologists. The annotations specifically focus on identifying the presence or absence of five distinct types of hematoma. The substantial scale of the dataset, coupled with the expertise reflected in the annotations, positions it as a valuable and comprehensive resource for the development and evaluation of machine-learning and deep-learning algorithms and models dedicated to hematoma detection and classification in the realm of medical imaging applications. The detailed annotations provided by expert radiologists contribute to the dataset's credibility and reliability, enabling the creation and refinement of sophisticated algorithms that can effectively navigate the intricacies of hematoma detection and classification. The types of intracranial hemorrhage are as follows

1. Intraparenchymal Hemorrhage (IPH)
2. Epidural Hemorrhage (EDH)
3. Subdural Hemorrhage (SDH)
4. Subarachnoid Hemorrhage (SAH)
5. Intraventricular Hemorrhage (IVH)

The training set consists of 752,803 images, and the test set consists of 121,232 images. The dataset has a class imbalance, meaning that some types of hematoma are more common than others shown in Figure 4.1. The class imbalance in the

RSNA dataset poses a noteworthy challenge, as certain types of hematoma are more prevalent than others.

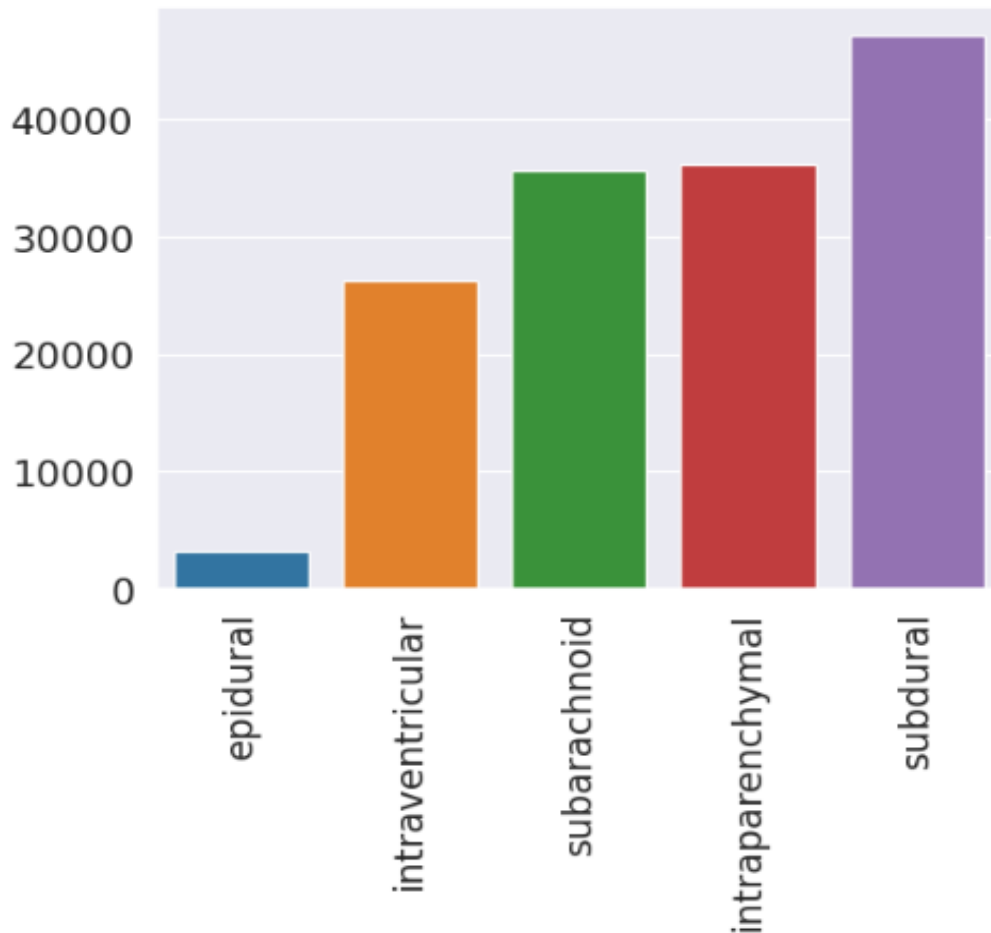


FIGURE 4.1: Class-wise Distribution

The dataset in question lacks any patient-specific clinical or medical details, rendering it ethically suitable for integration into this study. The absence of confidential or private patient information ensures that the dataset aligns with ethical guidelines, providing a secure foundation for analysis and research endeavors. The structure of the training data is organized such that each image ID is linked to multiple labels, encompassing the five distinct hemorrhage subtypes.

Additionally, there exists an extra label that remains consistently valid whenever any of the subtype labels are present. Each individual file is specifically annotated to signify the presence or absence of one or more types of hemorrhage, or alternatively, the complete absence of any hemorrhage indication. It is noteworthy

that the majority of scans within the dataset exhibit no discernible indications of hemorrhage. Facilitating the integration of labels with the corresponding images, a CSV (Comma-Separated Values) file was employed to provide information for each patient ID. This CSV file is structured to include six lines of information for every patient ID, contributing to the comprehensive annotation and categorization of the dataset for research purposes. These lines correspond to the different types of bleeding and employ a Boolean value to signify the presence or absence of a particular form of hemorrhage within the image. Shown In Figure 4.2.

id	subtype	any	epidural	intraparenchymal	intraventricular	subarachnoid	subdural
ID_00468a75e_aug120417	1	0	0	0	1	0	0
ID_004966d37_aug16897	1	1	1	1	1	0	0
ID_005362755_aug22305	1	0	1	1	1	0	0
ID_0082df059_aug45089	1	0	0	0	1	1	0
ID_0087b9306_aug92481	1	0	0	0	1	0	0
ID_0092877bb_aug57601	1	0	1	1	1	0	0
ID_009b2cf4a_aug37761	1	0	0	0	1	0	0
ID_00a26dc53_aug72065	1	0	0	0	1	1	0
ID_00a574cc6_aug91201	1	0	1	1	1	0	0
ID_00a7152b9_aug90113	1	0	0	0	1	1	1
ID_00bcb2785_aug36065	1	0	0	0	1	0	0
ID_00bcb2785_aug68673	1	0	0	0	1	0	0
ID_00c5876eb_aug109313	1	1	0	0	1	0	0
ID_00cb1a136_aug75393	1	0	1	1	1	0	0
ID_00cb73f69_aug105505	1	0	0	0	1	0	0
ID_00d298762_aug93697	1	0	1	1	1	0	0
ID_00e949dc7_aug44673	1	0	0	0	1	0	0

FIGURE 4.2: of the data frame where hemorrhage in the image

We have created two distinct datasets: Dataset 1 and Dataset 2. In Dataset 1, there are no mutually exclusive labels, and each DICOM file contains only one

type of hemorrhage or no hemorrhage at all.

In Dataset 2, we encounter mutually exclusive labels, where a single DICOM file can contain more than one type of hemorrhage or none at all. Notably, Epidural hemorrhages are underrepresented, with only 3,145 DICOM images in the dataset.

To address this class imbalance issue, we have chosen to exclude this type from our analysis and balance the data using the Augmentation technique. To augment our dataset effectively, we applied the Augmentation technique specifically to the Intraventricular Hemorrhage class. This process generated additional images.

In Dataset 1, we ensured that each class had a consistent count of 15,000 DICOM images, Shown in Figure 4.3 In Dataset 2, we aimed for each type to contain 30,000 DICOM images, but due to random selection, some duplicate files were introduced. After eliminating these duplicates, the revised counts are presented in Figure 4.4 for clarity.

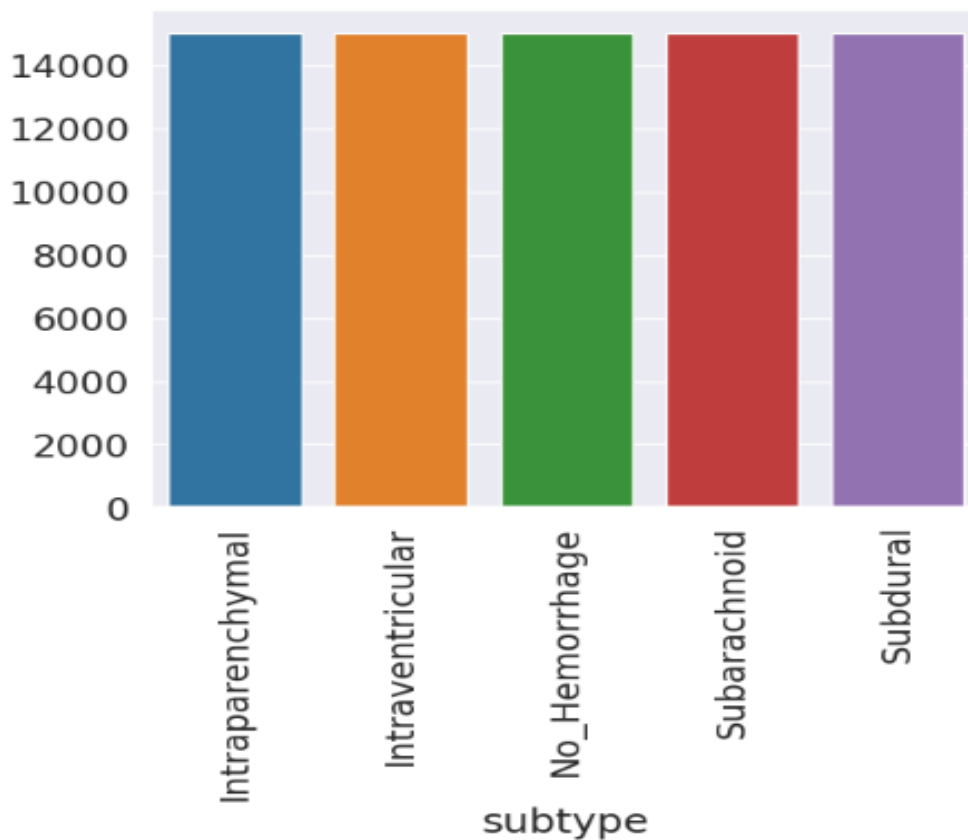


FIGURE 4.3: Balance Dataset1



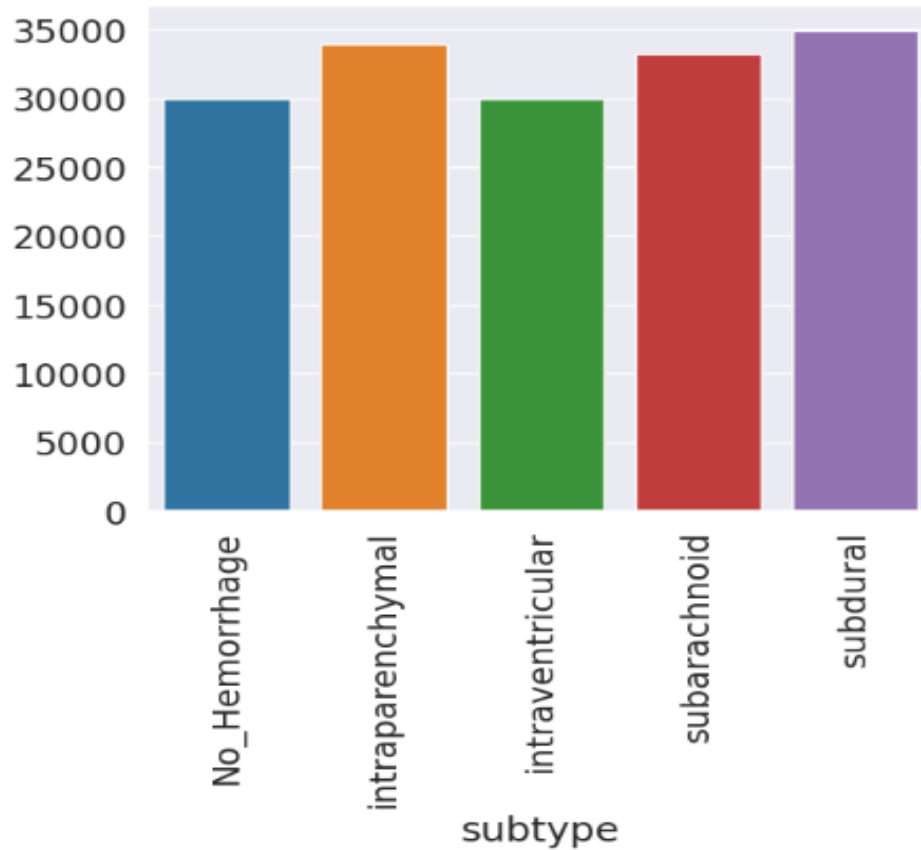


FIGURE 4.4: Balance Dataset2

### 4.3 Implementation of Model

The Attention U-Net model was implemented in TensorFlow and Keras libraries. The model consists of an encoder and a decoder. The encoder is a series of convolutional layers that extract features from the input image. The decoder is a series of convolutional layers that reconstruct the image from the features extracted by the encoder. The attention mechanism is used in the decoder to focus on the most important features of the image.

The encoder consists of five convolutional layers with 64, 128, 256, 512, and 1024 filters, respectively. Each convolutional layer is followed by a ReLU activation function and a max pooling layer with a 3x3 kernel and a stride of 2. The decoder consists of five convolutional layers with 1024, 512, 256, 128, and 64 filters, respectively. Each convolutional layer is followed by a ReLU activation function and an

upsampling layer with a 2x2 kernel and a stride of 2. The attention mechanism is implemented as a convolutional neural network with 64 filters. The convolutional neural network takes as input the features extracted by the encoder and the features extracted by the decoder. The output of the convolutional neural network is a gating signal that is used to weight the features extracted by the decoder.

TABLE 4.1: Model Parameter

Parameter	Value
Convolution Layer	18
Convolution Layer Filter	16
Convolution Layer Kernel Size	3
Convolution Layer Activation Function	Relu
Pooling Layer	5
Pooling Method	Max Pooling
Pooling Size	2
Skip Connection	4
Stride	2
Optimizer	Adam
Loss Function	Binary Cross Entropy
Batch Size	8
Epochs	32

Creating learning curves for both the training and validation sets is a crucial step in evaluating the performance of the Attention U-Net model. These curves provide insights into the model's training progress, revealing how its performance evolves over successive epochs. Typically, learning curves depict the model's loss and accuracy metrics on both the training and validation sets.

The loss curve illustrates the model's convergence during training. A decreasing loss indicates that the model is learning and improving its predictions. Meanwhile, the accuracy curve showcases the model's classification performance. Higher accuracy values indicate better performance, but it's essential to monitor both the training and validation curves to identify potential overfitting or underfitting issues. Examining the learning curves allows practitioners to make informed decisions

regarding model training, hyperparameter tuning, and potential adjustments to prevent overfitting or enhance generalization. It provides a visual representation of the trade-off between model complexity and its ability to generalize to new, unseen data.

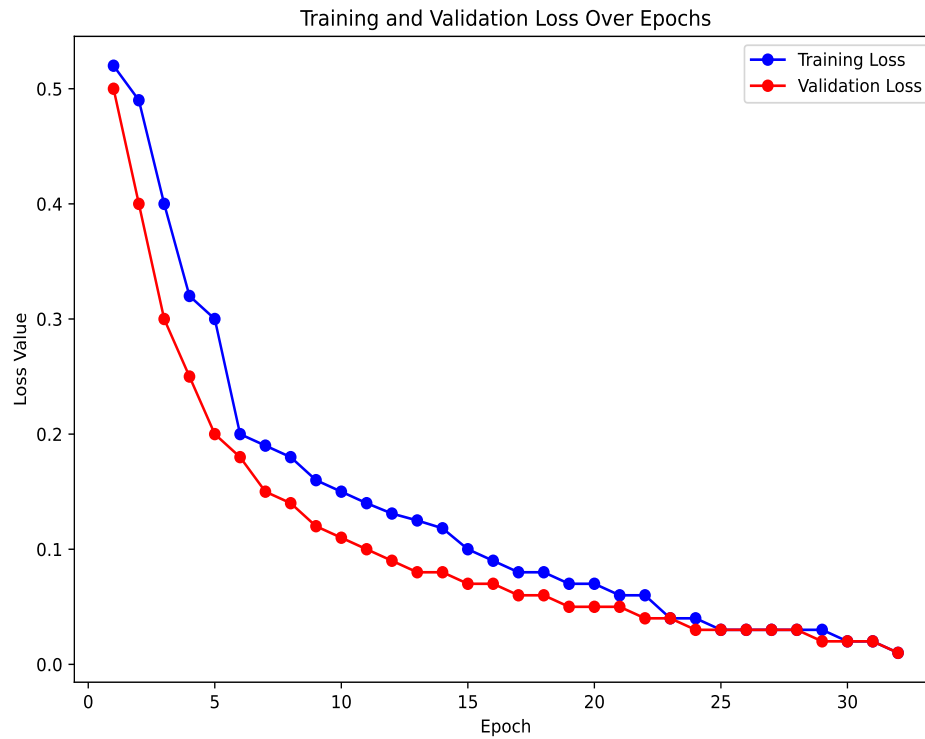


FIGURE 4.5: Train and Validation Learning Curves

## 4.4 Classification

In our dataset, there are no explicit segmentation masks available. Therefore, we employed an Attention-based U-Net model, which leverages attention gates to capture essential features without relying on explicit segmentation masks. At the conclusion of the Attention U-Net model, we obtain segmented images. Subsequently, we apply a classification layer to categorize these segmented images into different subtypes of intracranial hemorrhage. To assess the performance of our model, we utilized the average F1-score as a key evaluation metric. On Dataset 1, our model achieved an impressive average F1-score of 0.79, demonstrating its effectiveness in accurately classifying intracranial hemorrhage subtypes. Furthermore,

on Dataset 2, our model achieved a commendable average F1-score of 0.73, reaffirming its robustness in handling more challenging data scenarios. Additionally, our model succeeded in enhancing the accuracy of classification for each individual hemorrhage subtype.

TABLE 4.2: Class Wise Result of Dataset 1

Type Of Hemorrhage	Precision	Recall	F1 Score
Subdural	0.85	0.59	0.70
Subarachnoid	0.75	0.82	0.78
Intraventricular	0.92	0.88	0.90
Intraparenchymal	0.82	0.77	0.79
Normal Image	0.81	0.73	0.77

TABLE 4.3: Class Wise Result of Dataset 2

Type Of Hemorrhage	Precision	Recall	F1 Score
Subdural	0.84	0.41	0.55
Subarachnoid	0.93	0.71	0.80
Intraventricular	0.89	0.68	0.73
Intraparenchymal	0.85	0.84	0.84
Normal Image	0.78	0.63	0.70

## 4.5 Analysis of Result

In our comparative analysis, we considered five widely recognized benchmark models along with a state-of-the-art model that served as a reference point for our study. The outcomes, which are highlighted in bold and underlined, underscore the remarkable performance of our proposed model in contrast to the benchmark techniques. Specifically, our model achieved an outstanding accuracy of 92% on Dataset 1 and 87% on Dataset 2, marking the highest levels of accuracy across all benchmark studies. These results vividly illustrate the superior performance of our proposed model in intracranial hemorrhage subtype classification. For a visual

representation of the accuracy comparison between our model and the benchmark approaches. Moreover, the achieved F1 scores further underscore the efficacy of our proposed model, reaching an impressive 79% on Dataset 1 and 73% on Dataset 2. These robust F1 scores signify a balanced performance in terms of precision and recall, highlighting the model's capability to effectively classify intracranial hemorrhage subtypes across diverse datasets. This achievement solidifies the position of our proposed model as a top-performing solution in the challenging domain of medical image classification.

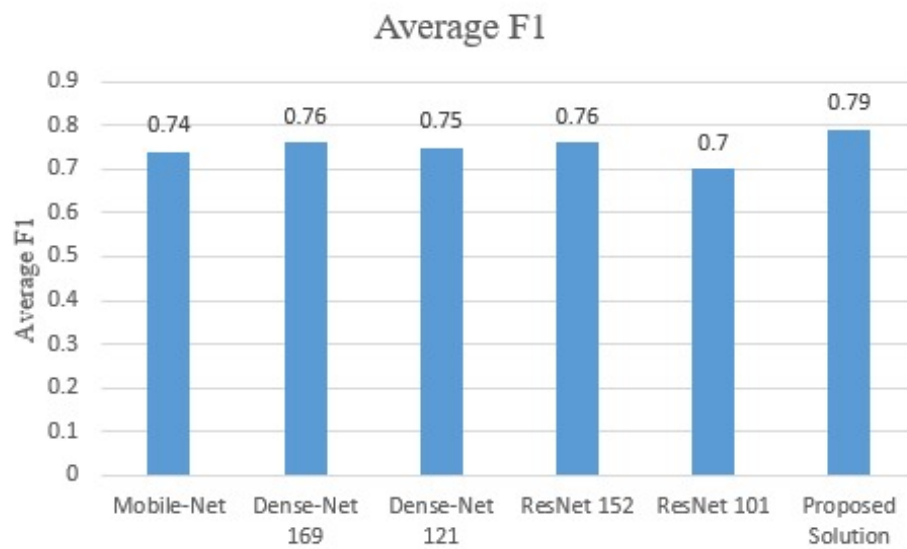


FIGURE 4.6: dataset 1 F-Score of different Techniques

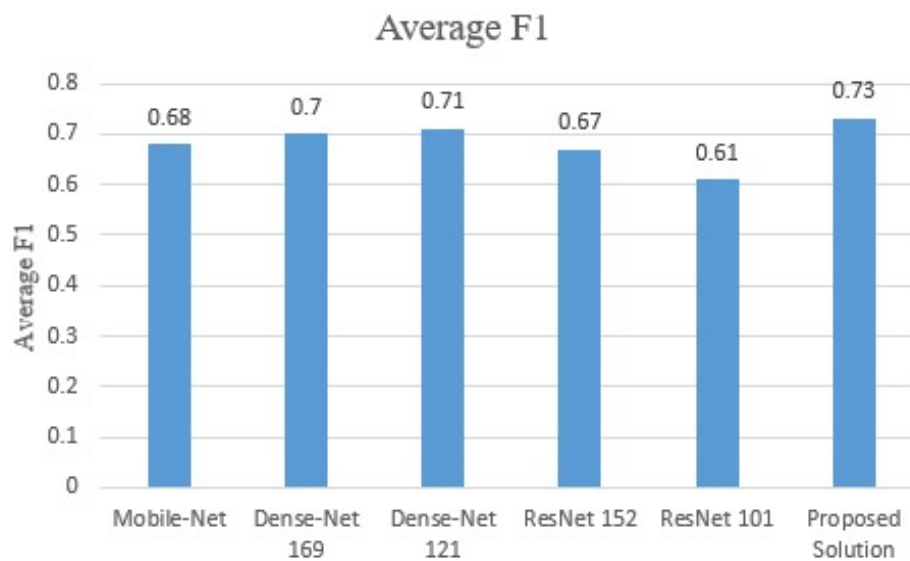


FIGURE 4.7: dataset 2 F-Score of different Techniques

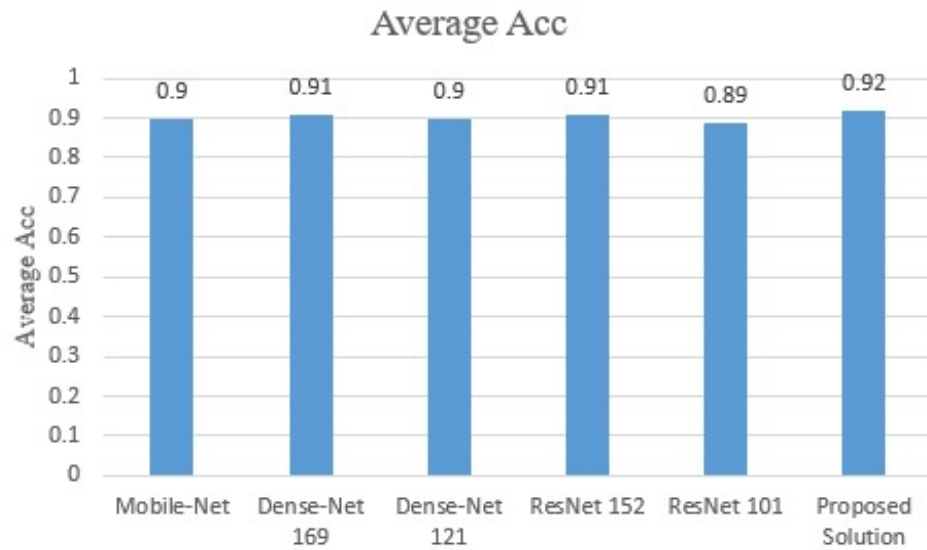


FIGURE 4.8: dataset 1 Accuracy of different Techniques

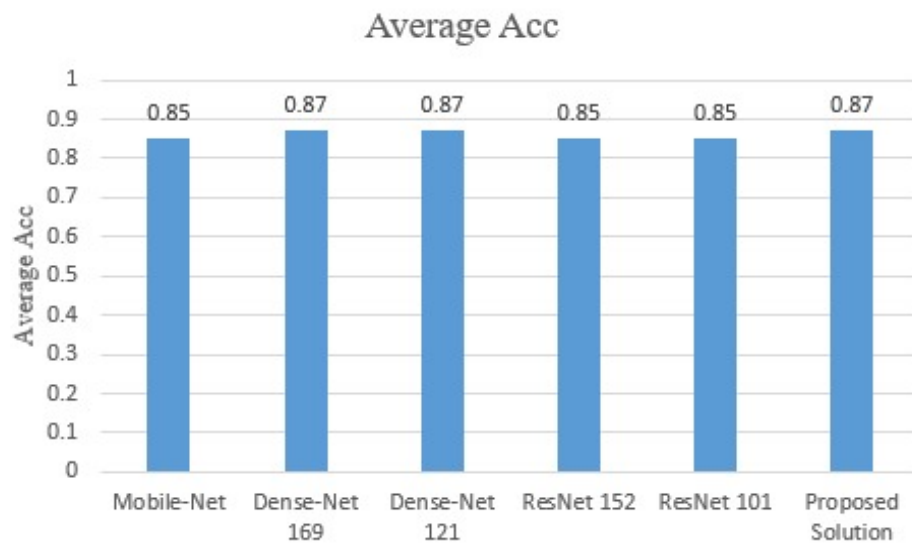


FIGURE 4.9: dataset 2 Accuracy of different Techniques

The Attention U-Net Model stands out prominently when compared to various benchmark models in the intricate task of classifying intracranial hemorrhages. In the evaluation using Dataset 1, it not only showcases superior performance but also achieves an outstanding F1-Score of 0.79. This remarkable F1-Score underscores the model's exceptional ability to strike a harmonious balance between precision and recall, a crucial aspect in medical image classification. Furthermore, the Attention U-Net Model attains the highest accuracy of 92%, indicating a commendable correctness in distinguishing between different subtypes of hemorrhages.

The robust performance of the model is further evident in its True Positive Rate (TPR) of 0.76, ensuring accurate identification of positive hemorrhage cases, and a notably high True Negative Rate (TNR) of 0.96. This high TNR signifies the model's proficiency in correctly recognizing cases without hemorrhage. The comprehensive comparative analysis unequivocally establishes the Attention U-Net Model as a standout choice for precise and accurate intracranial hemorrhage classification. Its superior metrics, encompassing F1-Score, accuracy, TPR, and TNR, solidify its position as a leading model in the challenging landscape of medical image analysis and classification. Beyond its remarkable metrics, what sets the Attention U-Net Model apart is its intricate understanding of image features, facilitated by the incorporation of attention gates. These attention gates endow the model with the capability to intelligently select and prioritize the most relevant features within the image data. This strategic feature selection ensures that the model excels at capturing critical information, avoiding being overwhelmed by irrelevant data.

A distinguishing feature of the Attention U-Net Model lies in its hierarchical feature extraction embedded within the U-Net framework, complemented by attention mechanisms. This combination enables the model to develop a profound understanding of image intricacies, spanning from low-level features like edges and corners to high-level features encompassing objects and shapes. This nuanced comprehension contributes to the model's ability to identify subtle nuances crucial for improved classification accuracy.

Moreover, the model seamlessly integrates segmentation and classification tasks within a unified framework. This cohesiveness results in enhanced feature representations, fostering a more holistic understanding of image data. This unique attribute ensures that the Attention U-Net Model is not only adept at identifying and prioritizing features for classification but also excels in the intricate task of segmentation.

In summary, the Attention U-Net Model's superiority extends beyond numerical metrics, encompassing its intelligent feature prioritization, nuanced image understanding, and seamless fusion of segmentation and classification tasks. These

qualities collectively position it as a leading choice for medical image analysis, particularly in the intricate domain of intracranial hemorrhage subtype classification.

TABLE 4.4: Comparison of Attention UNet Model using Dataset 1

Model	F1_avg	ACC_avg	TPR_avg	TNR_avg
Mobile-Net	0.74	0.90	0.70	0.95
Dense-Net 169	0.76	0.91	0.74	0.95
Dense-Net 121	0.75	0.90	0.72	0.95
ResNet 152	0.76	0.91	0.72	<b>0.96</b>
ResNet 101	0.70	0.89	0.68	0.94
Proposed Solution	<b>0.79</b>	<b>0.92</b>	<b>0.76</b>	<b>0.96</b>

TABLE 4.5: Comparison of Attention UNet Model using Dataset 2

Model	F1_avg	ACC_avg	TPR_avg	TNR_avg
Mobile-Net	0.68	0.85	0.58	<b>0.97</b>
Dense-Net 169	0.70	<b>0.87</b>	0.61	<b>0.97</b>
Dense-Net 121	0.71	<b>0.87</b>	0.60	0.96
ResNet 152	0.67	0.85	0.58	0.95
ResNet 101	0.69	0.85	0.59	0.96
Proposed Solution	<b>0.73</b>	<b>0.87</b>	<b>0.64</b>	0.95

## 4.6 Model Performance Analysis

The proposed model, built on the Attention U-Net architecture, has proven its superiority with the highest F1 score, recall, and precision values among the evaluated models. This outstanding performance is underpinned by several compelling factors. The Attention U-Net model’s integration of attention gates is a key element, enabling it to intelligently select and prioritize the most relevant features in image data, a crucial aspect for successful classification tasks. The attention gates serve as a mechanism that allows the model to focus on critical information



while avoiding being overwhelmed by irrelevant data, showcasing its adeptness in discerning salient aspects of the image.

Furthermore, the model's hierarchical feature extraction, seamlessly embedded within the U-Net framework alongside attention mechanisms, empowers it with a profound understanding of both low-level and high-level features in the image. This nuanced comprehension extends to subtle details, such as edges and corners, as well as more complex features like objects and shapes. This capability significantly contributes to the model's accuracy in identifying intricate nuances in the data. A standout attribute of the Attention U-Net model is its seamless integration of segmentation and classification tasks within a unified framework. This synergy between tasks results in enhanced feature representations, fostering a holistic understanding of the image data. The model's ability to discern and classify intracranial hemorrhage subtypes is thereby substantially strengthened.

In summary, the exceptional performance of the Attention U-Net model, as evidenced by its remarkable F1 scores, recall rates, and precision values, establishes it as the preeminent choice for image classification, particularly in the challenging domain of intracranial hemorrhage subtype classification. The model's diverse capabilities, ranging from feature prioritization to nuanced image understanding, solidify its position as a leader in the field of medical image analysis and classification.

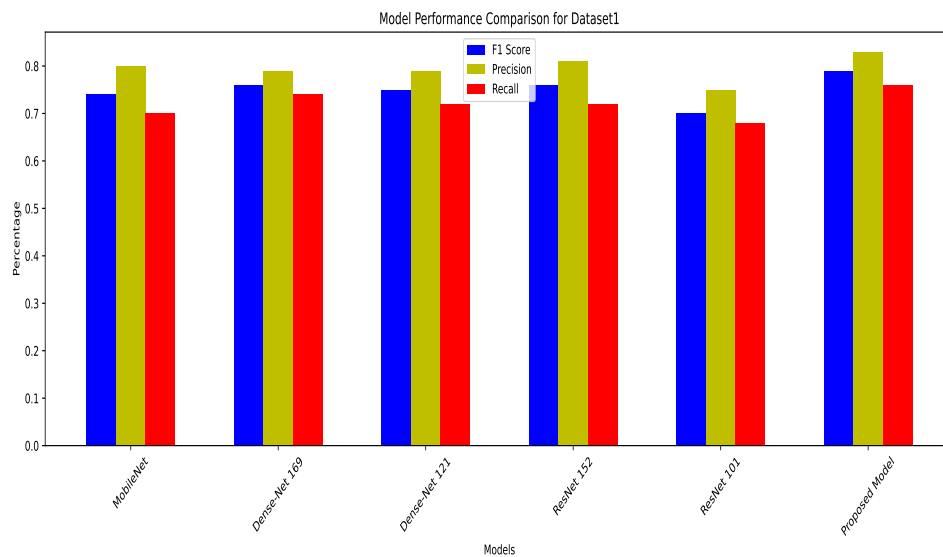


FIGURE 4.10: Dataset 1 Model Performance with different Techniques

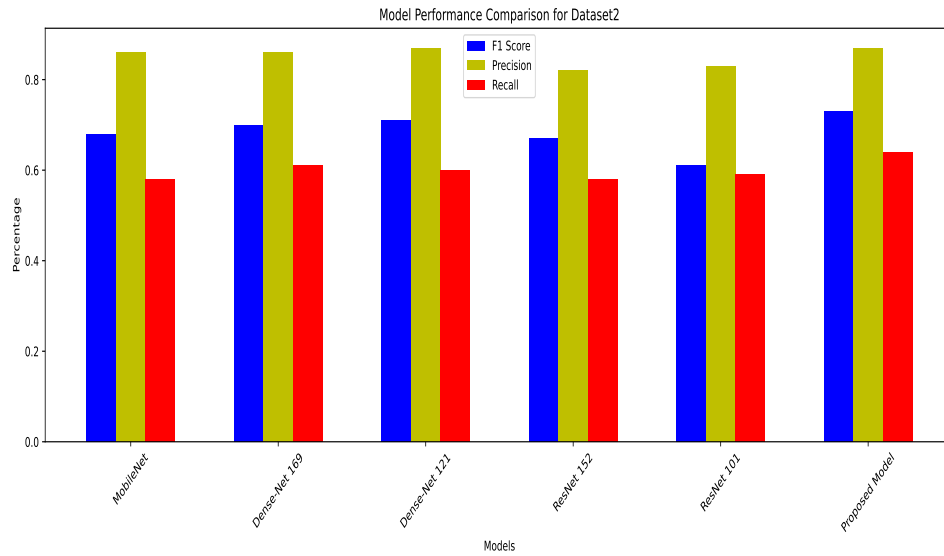


FIGURE 4.11: Dataset 2 Model Performance with different Techniques

## 4.7 Comparative Analysis

In the domain of intracranial hemorrhage classification, our approach integrates the innovative Attention UNet model with several existing methodologies. The performance evaluation is based on a set of robust metrics including the F1 score, average accuracy (ACC), true positive rate (TPR), and true negative rate (TNR).

Notably, among the pre-existing models, EfficientNet-b4 and EfficientNet-b5 exhibit commendable F1 scores, achieving 66.75% and 66.9%, respectively. Their high ACC values suggest solid all-round performance. In contrast, EfficientNet-b3, while achieving a noteworthy TPR of 57.0%, lags in F1 score.

However, our proposed solution surpasses all existing methods with an impressive F1 score of 0.79, reflecting superior accuracy in intracranial hemorrhage subtype classification. This model excels not only in F1 score but also in ACC, TPR, and TNR, reaching values of 0.92, 0.76, and 0.96, respectively. These results underscore the substantial enhancement brought by the Attention UNet model-based approach in intracranial hemorrhage classification, positioning it as a robust and highly effective solution for this critical medical task. Furthermore, our model is evaluated against popular deep learning architectures such as Resnet101,

Resnext101 32x8d, Se Resnext50 32x4d, Densenet121, Densenet161, and various versions of Efficientnet (b1, b2, b3, b4, b5). While these architectures demonstrate commendable performances in terms of F1 scores and accuracy, none outperforms our proposed solution based on the Attention U-Net model. The MSFE+WGSA+JFM method achieves a competitive F1 avg score of 74.6, indicating its proficiency in intracranial hemorrhage classification. Nevertheless, our proposed Attention U-Net model surpasses it with an F1 avg score of 0.79, underscoring its superior performance. This remarkable outcome highlights the effectiveness of the attention-based approach in capturing crucial features and elevating classification accuracy. The superiority of the Attention UNet model can be attributed to several factors, including its use of attention gates for feature selection, allowing it to concentrate on essential information. Additionally, the combination of segmentation and classification within a single model enhances feature representations and, consequently, elevates classification accuracy. The hierarchical feature extraction within the U-Net architecture, complemented by attention mechanisms, fosters a more nuanced comprehension of image details and their relevance to classification. These combined strengths collectively contribute to the model's exceptional performance in comparison to other architectures and methods.

TABLE 4.6: Comparative Analysis with Current Approaches

Model	F1_avg	ACC_avg	TPR_avg	TNR_avg
Resnet101	58.6	97.2	50.6	99.30
Resnext101 32x8d	66.2	97.5	59.7	99.25
Se Resnext50 32x4d	58.4	97.2	52.0	99.21
Densenet121	57.1	97.2	49.3	99.23
Densenet161	58.8	97.2	52.0	99.22
Efficientnet-b1	56.1	97.2	47.4	99.43
Efficientnet-b2	57.1	97.2	49.3	99.21
Efficientnet-b3	65.3	97.6	57.0	99.42
Efficientnet-b4	66.75	97.5	61.8	99.11
Efficientnet-b5	66.9	97.5	62.8	99.0
MSFE+WGSA+JFM	74.6	98.1	68.4	99.28
Proposed Solution	<b>79</b>	92	<b>76</b>	96

# Chapter 5

## Conclusion and Future Work

### 5.1 Conclusion

In conclusion, our Attention U-Net model for intracranial hemorrhage classification has shown remarkable promise in accurately identifying and classifying different subtypes of hemorrhages from CT images. This model leverages the power of attention mechanisms to focus on critical features in the images, significantly enhancing its performance.

Our key findings and contributions include achieving an outstanding average F1-score of 0.79 on Dataset 1 and 0.73 on Dataset 2, along with improved accuracy for each subtype. In fact, our model outperformed several benchmark techniques, reaching an impressive accuracy of 92% on Dataset 1 and 87% on Dataset 2, marking it as the top-performing model in this context. Furthermore, our approach addresses challenges related to class imbalance, intricate label scenarios, and the absence of explicit segmentation masks. The incorporation of attention gates in the U-Net architecture signifies a significant advancement, enabling the model to make more informed decisions about feature emphasis. This enhancement not only contributes to accurate classification but also opens avenues for applications demanding high-quality segmentation results. Our meticulous dataset creation, balancing, and preprocessing strategies lay a robust foundation for model

training and analysis. The thoughtful design of two distinct datasets, each addressing specific label scenarios, reflects a nuanced exploration of different scenarios, providing valuable insights into challenges associated with mutually exclusive labels in medical image datasets.

The versatility of our methodology is exemplified by its ability to perform classification tasks without the need for manual segmentation annotations, making it applicable to a broader range of medical imaging datasets and scenarios. The Attention U-Net model's ability to seamlessly blend segmentation and classification tasks within a unified framework further enhances its suitability for diverse medical image analysis applications.

As for future work, there are several exciting avenues to explore:

1. **Data Augmentation:** Further enhancing the dataset with diverse augmentation techniques can potentially improve the model's robustness and generalization.
2. **Ensemble Learning:** Investigating the benefits of ensemble learning by combining multiple models or variations of the Attention U-Net can potentially yield even better results.
3. **Explainability:** Exploring methods for making the model's predictions more interpretable, especially in medical contexts, can help build trust with healthcare professionals.
4. **Real-Time Applications:** Adapting the model for real-time applications, such as assisting radiologists in diagnosing intracranial hemorrhages during CT scans, would be a significant step forward.
5. **Integration with Healthcare Systems:** Working towards integrating the model into existing healthcare systems to provide valuable support to medical professionals.

In conclusion, our Attention U-Net model has demonstrated its potential in improving intracranial hemorrhage classification, and there are exciting opportunities for further research and applications in the field of medical image analysis.

# Bibliography

- [1] N. S. Rost, A. Brodtmann, M. P. Pase, S. J. van Veluw, A. Biffi, M. Duerling, J. D. Hinman, and M. Dichgans, “Post-stroke cognitive impairment and dementia,” *Circulation Research*, vol. 130, no. 8, pp. 1252–1271, 2022.
- [2] V. L. Feigin, M. Brainin, B. Norrving, S. Martins, R. L. Sacco, W. Hacke, M. Fisher, J. Pandian, and P. Lindsay, “World stroke organization (wso): global stroke fact sheet 2022,” *International Journal of Stroke*, vol. 17, no. 1, pp. 18–29, 2022.
- [3] X. Ma, Y. Cheng, R. Garcia, and J. Haorah, “Hemorrhage associated mechanisms of neuroinflammation in experimental traumatic brain injury,” *Journal of Neuroimmune Pharmacology*, vol. 15, pp. 181–195, 2020.
- [4] J. A. Caceres and J. N. Goldstein, “Intracranial hemorrhage,” *Emergency medicine clinics of North America*, vol. 30, no. 3, pp. 771–794, 2012.
- [5] J. J. Heit, M. Iv, and M. Wintermark, “Imaging of intracranial hemorrhage,” *Journal of stroke*, vol. 19, no. 1, p. 11, 2017.
- [6] R. A. Rava, S. E. Seymour, M. E. LaQue, B. A. Peterson, K. V. Snyder, M. Mokin, M. Waqas, Y. Hoi, J. M. Davies, E. I. Levy *et al.*, “Assessment of an artificial intelligence algorithm for detection of intracranial hemorrhage,” *World Neurosurgery*, vol. 150, pp. e209–e217, 2021.
- [7] S. E. Arman, S. S. Rahman, N. Irtisam, S. A. Deowan, M. A. Islam, S. Sakib, and M. Hasan, “Intracranial hemorrhage classification from ct scan using deep learning and bayesian optimization,” *IEEE Access*, 2023.

- 
- [8] A. Barman, V. Lopez-Rivera, S. Lee, F. S. Vahidy, J. Z. Fan, S. I. Savitz, S. A. Sheth, and L. Giancardo, “Combining symmetric and standard deep convolutional representations for detecting brain hemorrhage,” in *Medical imaging 2020: Computer-aided diagnosis*, vol. 11314. SPIE, 2020, pp. 75–81.
- [9] L. Zhang, W. Miao, C. Zhu, Y. Wang, Y. Luo, R. Song, L. Liu, and J. Yang, “A weakly supervised-guided soft attention network for classification of intracranial hemorrhage,” *IEEE Transactions on Cognitive and Developmental Systems*, vol. 15, no. 1, pp. 42–53, 2022.
- [10] Ö. F. Ertuğrul and M. F. Akıl, “Detecting hemorrhage types and bounding box of hemorrhage by deep learning,” *Biomedical Signal Processing and Control*, vol. 71, p. 103085, 2022.
- [11] J. Vymazal, A. M. Rulseh, J. Keller, and L. Janouskova, “Comparison of ct and mr imaging in ischemic stroke,” *Insights into imaging*, vol. 3, no. 6, pp. 619–627, 2012.
- [12] R. A. Castellino, “Computer aided detection (cad): an overview,” *Cancer Imaging*, vol. 5, no. 1, p. 17, 2005.
- [13] R. Karthik, R. Menaka, A. Johnson, and S. Anand, “Neuroimaging and deep learning for brain stroke detection—a review of recent advancements and future prospects,” *Computer Methods and Programs in Biomedicine*, vol. 197, p. 105728, 2020.
- [14] K. R. Bhatele and S. S. Bhadauria, “Brain structural disorders detection and classification approaches: a review,” *Artificial Intelligence Review*, vol. 53, pp. 3349–3401, 2020.
- [15] A. Gudigar, U. Raghavendra, A. Hegde, M. Kalyani, E. J. Ciaccio, and U. R. Acharya, “Brain pathology identification using computer aided diagnostic tool: A systematic review,” *Computer Methods and Programs in Biomedicine*, vol. 187, p. 105205, 2020.
- [16] K. P. Murphy, *Machine learning: a probabilistic perspective*. MIT press, 2012.

- [17] M. Sonka, V. Hlavac, and R. Boyle, *Image processing, analysis, and machine vision*. Cengage Learning, 2014.
- [18] X. Wang and K. K. Paliwal, “Feature extraction and dimensionality reduction algorithms and their applications in vowel recognition,” *Pattern recognition*, vol. 36, no. 10, pp. 2429–2439, 2003.
- [19] A. M. Dawud, K. Yurtkan, H. Oztoprak *et al.*, “Application of deep learning in neuroradiology: brain haemorrhage classification using transfer learning,” *Computational Intelligence and Neuroscience*, vol. 2019, 2019.
- [20] D. Erhan, A. Courville, Y. Bengio, and P. Vincent, “Why does unsupervised pre-training help deep learning?” in *Proceedings of the thirteenth international conference on artificial intelligence and statistics*. JMLR Workshop and Conference Proceedings, 2010, pp. 201–208.
- [21] D. Cireşan, U. Meier, J. Masci, and J. Schmidhuber, “A committee of neural networks for traffic sign classification,” in *The 2011 international joint conference on neural networks*. IEEE, 2011, pp. 1918–1921.
- [22] U. Raghavendra, H. Fujita, S. V. Bhandary, A. Gudigar, J. H. Tan, and U. R. Acharya, “Deep convolution neural network for accurate diagnosis of glaucoma using digital fundus images,” *Information Sciences*, vol. 441, pp. 41–49, 2018.
- [23] A. Sage and P. Badura, “Intracranial hemorrhage detection in head ct using double-branch convolutional neural network, support vector machine, and random forest,” *Applied Sciences*, vol. 10, no. 21, p. 7577, 2020.
- [24] C. W. Anouk Stein, MD, “Rsna intracranial hemorrhage detection,” 2019. [Online]. Available: <https://kaggle.com/competitions/rsna-intracranial-hemorrhage-detection>
- [25] O. Oktay, J. Schlemper, L. L. Folgoc, M. Lee, M. Heinrich, K. Misawa, K. Mori, S. McDonagh, N. Y. Hammerla, B. Kainz *et al.*, “Attention u-net: Learning where to look for the pancreas,” *arXiv preprint arXiv:1804.03999*, 2018.



- [26] V. García-Blázquez, A. Vicente-Bártulos, A. Olavarria-Delgado, M. Plana, D. Van Der Winden, J. Zamora, and E.-C. Collaboration, “Accuracy of ct angiography in the diagnosis of acute gastrointestinal bleeding: systematic review and meta-analysis,” *European radiology*, vol. 23, pp. 1181–1190, 2013.
- [27] H. R. Bello, J. A. Graves, S. Rohatgi, M. Vakil, J. McCarty, R. L. Van Hemert, S. Geppert, and R. B. Peterson, “Skull base-related lesions at routine head ct from the emergency department: pearls, pitfalls, and lessons learned,” *Radiographics*, vol. 39, no. 4, pp. 1161–1182, 2019.
- [28] U. Raghavendra, T.-H. Pham, A. Gudigar, V. Vidhya, B. N. Rao, S. Sabut, J. K. E. Wei, E. J. Ciaccio, and U. R. Acharya, “Novel and accurate non-linear index for the automated detection of haemorrhagic brain stroke using ct images,” *Complex & Intelligent Systems*, vol. 7, pp. 929–940, 2021.
- [29] M. Grewal, M. M. Srivastava, P. Kumar, and S. Varadarajan, “Radnet: Radiologist level accuracy using deep learning for hemorrhage detection in ct scans,” in *2018 IEEE 15th International Symposium on Biomedical Imaging (ISBI 2018)*. IEEE, 2018, pp. 281–284.
- [30] M. R. Arbabshirani, B. K. Fornwalt, G. J. Mongelluzzo, J. D. Suever, B. D. Geise, A. A. Patel, and G. J. Moore, “Advanced machine learning in action: identification of intracranial hemorrhage on computed tomography scans of the head with clinical workflow integration,” *NPJ digital medicine*, vol. 1, no. 1, p. 9, 2018.
- [31] J. Cho, K.-S. Park, M. Karki, E. Lee, S. Ko, J. K. Kim, D. Lee, J. Choe, J. Son, M. Kim *et al.*, “Improving sensitivity on identification and delineation of intracranial hemorrhage lesion using cascaded deep learning models,” *Journal of digital imaging*, vol. 32, pp. 450–461, 2019.
- [32] H. Ye, F. Gao, Y. Yin, D. Guo, P. Zhao, Y. Lu, X. Wang, J. Bai, K. Cao, Q. Song *et al.*, “Precise diagnosis of intracranial hemorrhage and subtypes using a three-dimensional joint convolutional and recurrent neural network,” *European radiology*, vol. 29, pp. 6191–6201, 2019.

- [33] A. Bar, M. M. Havakuk, Y. Turner, M. Safadi, and E. Elnekave, “Improved ich classification using task-dependent learning,” in *2019 IEEE 16th International Symposium on Biomedical Imaging (ISBI 2019)*. IEEE, 2019, pp. 1567–1571.
- [34] J. He, “Automated detection of intracranial hemorrhage on head computed tomography with deep learning,” in *Proceedings of the 2020 10th international conference on biomedical engineering and technology*, 2020, pp. 117–121.
- [35] D. Guo, H. Wei, P. Zhao, Y. Pan, H.-Y. Yang, X. Wang, J. Bai, K. Cao, Q. Song, J. Xia *et al.*, “Simultaneous classification and segmentation of intracranial hemorrhage using a fully convolutional neural network,” in *2020 IEEE 17th International Symposium on Biomedical Imaging (ISBI)*. IEEE, 2020, pp. 118–121.
- [36] M. Hssayeni, M. Croock, A. Salman, H. Al-khafaji, Z. Yahya, and B. Gho-raani, “Computed tomography images for intracranial hemorrhage detection and segmentation,” *Intracranial Hemorrhage Segmentation Using A Deep Convolutional Model. Data*, vol. 5, no. 1, p. 14, 2020.
- [37] J. Mantas *et al.*, “Classification of intracranial hemorrhage subtypes using deep learning on ct scans,” *The Importance of Health Informatics in Public Health during a Pandemic*, vol. 272, p. 370, 2020.
- [38] H. Ko, H. Chung, H. Lee, and J. Lee, “Feasible study on intracranial hemorrhage detection and classification using a cnn-lstm network,” in *2020 42nd Annual International Conference of the IEEE Engineering in Medicine & Biology Society (EMBC)*. IEEE, 2020, pp. 1290–1293.
- [39] R. F. Mansour and N. O. Aljehane, “An optimal segmentation with deep learning based inception network model for intracranial hemorrhage diagnosis,” *Neural Computing and Applications*, vol. 33, no. 20, pp. 13 831–13 843, 2021.
- [40] Y. Watanabe, T. Tanaka, A. Nishida, H. Takahashi, M. Fujiwara, T. Fujiwara, A. Arisawa, H. Yano, N. Tomiyama, H. Nakamura *et al.*, “Improvement of the

- diagnostic accuracy for intracranial haemorrhage using deep learning-based computer-assisted detection,” *Neuroradiology*, vol. 63, pp. 713–720, 2021.
- [41] G. Zhang, K. Chen, S. Xu, P. C. Cho, Y. Nan, X. Zhou, C. Lv, C. Li, and G. Xie, “Lesion synthesis to improve intracranial hemorrhage detection and classification for ct images,” *Computerized Medical Imaging and Graphics*, vol. 90, p. 101929, 2021.
- [42] I. Kumar, C. Bhatt, and K. U. Singh, “Entropy based automatic unsupervised brain intracranial hemorrhage segmentation using ct images,” *Journal of King Saud University-Computer and Information Sciences*, vol. 34, no. 6, pp. 2589–2600, 2022.
- [43] C. Anupama, M. Sivaram, E. L. Lydia, D. Gupta, and K. Shankar, “Synergic deep learning model-based automated detection and classification of brain intracranial hemorrhage images in wearable networks,” *Personal and Ubiquitous Computing*, pp. 1–10, 2022.
- [44] M. Ganeshkumar, V. Ravi, V. Sowmya, E. Gopalakrishnan, K. Soman, and C. Chakraborty, “Identification of intracranial haemorrhage (ich) using resnet with data augmentation using cyclegan and ich segmentation using segan,” *Multimedia Tools and Applications*, vol. 81, no. 25, pp. 36 257–36 273, 2022.
- [45] S. Nizarudeen and G. R. Shunmugavel, “Multi-layer resnet-densenet architecture in consort with the xgboost classifier for intracranial hemorrhage (ich) subtype detection and classification,” *Journal of Intelligent & Fuzzy Systems*, no. Preprint, pp. 1–16, 2023.
- [46] L. Cortés-Ferre, M. A. Gutiérrez-Naranjo, J. J. Egea-Guerrero, S. Pérez-Sánchez, and M. Balcerzyk, “Deep learning applied to intracranial hemorrhage detection,” *Journal of Imaging*, vol. 9, no. 2, p. 37, 2023.
- [47] S. E. Arman, S. S. Rahman, N. Irtisam, S. A. Deowan, M. A. Islam, S. Sakib, and M. Hasan, “Intracranial hemorrhage classification from ct scan using deep learning and bayesian optimization,” *IEEE Access*, 2023.

- 
- [48] J. Ker, S. P. Singh, Y. Bai, J. Rao, T. Lim, and L. Wang, “Image thresholding improves 3-dimensional convolutional neural network diagnosis of different acute brain hemorrhages on computed tomography scans,” *Sensors*, vol. 19, no. 9, p. 2167, 2019.
- [49] A.-C. Phan, V.-Q. Vo, and T.-C. Phan, “Automatic detection and classification of brain hemorrhages,” in *Asian Conference on Intelligent Information and Database Systems*. Springer, 2018, pp. 417–427.
- [50] A. Majumdar, L. Brattain, B. Telfer, C. Farris, and J. Scalera, “Detecting intracranial hemorrhage with deep learning,” in *2018 40th annual international conference of the IEEE engineering in medicine and biology society (EMBC)*. IEEE, 2018, pp. 583–587.
- [51] H. Lee, S. Yune, M. Mansouri, M. Kim, S. H. Tajmir, C. E. Guerrier, S. A. Ebert, S. R. Pomerantz, J. M. Romero, S. Kamalian *et al.*, “An explainable deep-learning algorithm for the detection of acute intracranial haemorrhage from small datasets,” *Nature biomedical engineering*, vol. 3, no. 3, pp. 173–182, 2019.

## Turnitin Originality Report

A Deep Learning Framework for Classification of Intracranial Hemorrhage Subtypes with Attention-Based Approaches by Memoona Zulfiqar

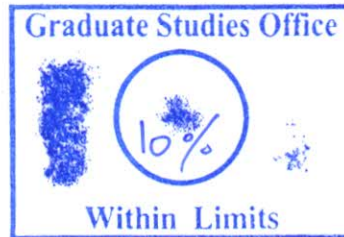


From Ms Theses (CUST Library)

- Processed on 16-Nov-2023 12:02 PKT
- ID: 2229889384
- Word Count: 19040

Similarity Index  
10%  
Similarity by Source

Internet Sources:  
5%  
Publications:  
7%  
Student Papers:  
2%



## sources:

- 1 1% match (Internet from 19-Aug-2022)

[https://www.researchgate.net/publication/342882230\\_Automatic\\_segmentation\\_of\\_intracerebral\\_hemorrhage\\_in\\_CT\\_images\\_using\\_decoder\\_convolutional\\_neural\\_network](https://www.researchgate.net/publication/342882230_Automatic_segmentation_of_intracerebral_hemorrhage_in_CT_images_using_decoder_convolutional_neural_network)

- 2 1% match (Shanu Nizarudeen, Ganesh Ramaswamy Shanmughavel. "Comparative analysis of ResNet, ResNet-SE, and attention-based RaNet for hemorrhage classification in CT images using deep learning", Biomedical Signal Processing and Control, 2024)

[Shanu Nizarudeen, Ganesh Ramaswamy Shanmughavel. "Comparative analysis of ResNet, ResNet-SE, and attention-based RaNet for hemorrhage classification in CT images using deep learning". Biomedical Signal Processing and Control, 2024](#)

- 3 1% match (student papers from 03-Oct-2018)

[Submitted to Bacha Khan University, Charsada on 2018-10-03](#)

- 4 1% match (Jiajie He. "Automated Detection of Intracranial Hemorrhage on Head Computed Tomography with Deep Learning", Proceedings of the 2020 10th International Conference on Biomedical Engineering and Technology, 2020)

[Jiajie He. "Automated Detection of Intracranial Hemorrhage on Head Computed Tomography with Deep Learning". Proceedings of the 2020 10th International Conference on Biomedical Engineering and Technology, 2020](#)

- 5 < 1% match (Internet from 01-Feb-2023)

[https://www.researchgate.net/publication/333514712\\_Automated\\_brain\\_histology\\_classification\\_using\\_machine\\_learning](https://www.researchgate.net/publication/333514712_Automated_brain_histology_classification_using_machine_learning)

- 6 < 1% match (Internet from 28-Dec-2022)

[https://www.researchgate.net/publication/366605175\\_Colorization\\_Technique\\_to\\_improve\\_DCNN-based\\_ICH\\_CT\\_Image\\_Classification](https://www.researchgate.net/publication/366605175_Colorization_Technique_to_improve_DCNN-based_ICH_CT_Image_Classification)

- 7 < 1% match (Internet from 12-Aug-2022)

[https://www.researchgate.net/publication/357845144\\_Internet\\_of\\_things\\_and\\_wearables-enabled\\_Alzheimer\\_detection\\_and\\_classification\\_model\\_using\\_stacked\\_sparse\\_autoencoder](https://www.researchgate.net/publication/357845144_Internet_of_things_and_wearables-enabled_Alzheimer_detection_and_classification_model_using_stacked_sparse_autoencoder)

- 8 < 1% match ("Image Analysis and Processing. ICIAP 2022 Workshops", Springer Science and Business Media LLC, 2022)

["Image Analysis and Processing. ICIAP 2022 Workshops", Springer Science and Business Media LLC, 2022](#)

- 9 < 1% match (Shanu Nizarudeen, Ganesh R. Shunmugavel. "Multi-Layer ResNet-DenseNet architecture in consort with the XgBoost classifier for intracranial hemorrhage (ICH) subtype detection and classification", Journal of Intelligent & Fuzzy Systems, 2023)